POLITECNICO
MILANO 1863

SCHOOL OF CIVIL, ENVIRONMENTAL AND LAND MANAGEMENT ENGINEERING
MASTER OF SCIENCE IN ENVIRONMENTAL AND LAND PLANNING ENGINEERING

ANALYSIS OF THE INFLUENCE OF A DENSE NETWORK OF SMALL RESERVOIRS ON DROUGHT EVOLUTION

Master Thesis by:
Paolo Colombo
Matr. 928725

Advisor:
Prof. Andrea Castelletti

Co-Advisor:
Prof. Pieter Van Oel
MSc Germano Gondim Ribeiro Neto
Prof. Dr. rer. nat. Alexandre C. Costa

Academic Year 2020 – 2021

Acknowledgements

This study has been possible thanks to the cooperation and collaboration from Prof. Pieter van Oel, MSc Germano G. Ribeiro Neto (Wageningen University & Research, *The Netherlands*) and Prof. Andrea Castelletti (Politecnico di Milano, *Italy*), who all provided supervision and advice across the thesis' process. Alexandre C. Costa and George Mamede (UNILAB, *Brazil*) provided fundamental help in understanding and operating the WASA-SED model, aside from useful and important advice on the thesis itself. For this example of positive and fruitful collaboration I thank them all.
For helping me define the way I thank Cecilia, compass and parachute. For the support during the Dutch months and beyond I thank my family, Lorenzo, Sara and the 2A corridor. For the past, the present and the future I thank every person I was lucky enough to meet.

Abstract

In semi-arid regions, as a drought preparedness measure, small and medium reservoirs to collect and store water for local usage have been built with increased frequency in the last decades, forming what can be called a Dense Reservoir Network (DRN). Despite the capacity of this network being relatively small compared to the usual capacity of the centralized reservoirs, its presence creates a number of challenges for water management in the region. The vast majority of these reservoirs are unmonitored and most are unregistered, implying few possibilities to consider them in an integrated management of water resources. Moreover, their accumulated effects on the monitored and directly managed centralized reservoirs are still unclear, leaving questions about their influence in hydrological drought evolution both in time and in space.

This study considers this network by modeling two scenarios through a meso-scale semi-distributed hydrological model: one simulating the real situation with the presence of the DRN and another one simulating a condition without the DRN. Their differences in time and space are analyzed to investigate the effects generated by the presence of the network, considering also the uncertainties of the process. Other scenarios are considered to have a broader view. The Banabuiú river basin in the semiarid region of North-East Brazil is the case study, which in its 19,530 km^2 area presents both a network of centralized and controlled reservoirs and a dense network of small reservoirs.

Results show that the presence of the DRN accelerates the transition from meteorological towards hydrological drought phases and lengthens the recharge period in centralized reservoirs. The drought events become longer: the number of months in an hydrological drought condition is increased by 4%. At the same time the DRN increases the water storage capacity distribution throughout the basin, while the stored volume distribution still depends on large reservoirs. Possibilities are open to deepen the study of these influences, for example considering other drivers and cooperation in the management of large and small reservoirs.

Riassunto

In regioni semi-aride, come misura di prevenzione e adattamento alle siccità, negli ultimi decenni sono stati costruiti con sempre maggiore frequenza serbatoi piccoli e medi per raccogliere e immagazzinare l'acqua per uso locale, formando quella che può essere definita una densa rete di serbatoi (DRN: Dense Reservoir Network). Nonostante la capacità di questa rete sia relativamente bassa rispetto alla capacità dei serbatoi centralizzati, la sua presenza genera una serie di sfide per la gestione dell'acqua nella regione. La grande maggioranza di questi serbatoi non è monitorata e la maggior parte non è registrata, rendendo difficile quindi considerarli in una gestione integrata delle risorse idriche. Inoltre, i loro effetti cumulativi sui serbatoi centralizzati monitorati e gestiti direttamente non sono ancora chiari, lasciando domande sull'influenza della rete nell'evoluzione delle siccità idrologiche sia nel tempo che nello spazio.

Questo studio considera questa rete modellando due scenari attraverso un modello idrologico a mesoscala semi-distribuito: uno che simula la situazione reale con la presenza della DRN e un altro che simula una condizione senza la DRN. Le loro differenze nel tempo e nello spazio sono analizzate per indagare gli effetti generati dalla presenza della rete, considerando anche le incertezze del processo. Altri scenari sono considerati per avere una visione più ampia. Il caso di studio è il bacino del fiume Banabuiú nella regione semiarida del Brasile nord-orientale, che nella sua area di 19.530 km^2 presenta sia una rete di serbatoi centralizzati e controllati sia una fitta rete di piccoli serbatoi.

I risultati mostrano che la presenza della DRN accelera la transizione dalla fase di siccità meteorologica a quella idrologica e allunga il periodo di ricarica nei serbatoi centralizzati. Gli eventi di siccità si allungano: il numero di mesi in una condizione di siccità idrologica aumenta del 4%. Allo stesso tempo la DRN permette una capacità di stoccaggio dell'acqua più diffusa nel bacino, mentre la distribuzione del volume immagazzinato dipende ancora dai grandi serbatoi. Sono aperte ulteriori possibilità per approfondire lo studio di queste influenze, per esempio considerando altri fattori di impatto e la cooperazione nella gestione di grandi e piccoli serbatoi.

Contents

List of Figures

List of Tables

1 Introduction

The goal of this Chapter is to briefly describe the context of the study area and the problem statement that inspired this study. In Section 1.1, focusing on the greater semi-arid area of North-East Brazil (NEB) for the climatology and then on the actual study area of Banabuiú's river basin for the morphology. In Section 1.2 the premises and the rationale of this study are explained.

1.1 Context

1.1.1 Semiarid region of North-East Brazil

The study area (Banabuiú basin) is a catchment located in Brazil, specifically in the state of Ceará, in the North-East region of Brazil (NEB), shown in Figure 1.1. North-East Brazil's boundaries include the Brazilian federate states of Alagoas, Bahia, Maranhão, Paraíba, Pernambuco, Piauí, Rio Grande do Norte, Sergipe, and the aforementioned Ceará, although the Regional Division of Brazil is subjected to changes and revisions (IBGE, 2017). It covers a surface of 1,542,000 km^2, about 18.26% of Brazil's total area (Marengo et al., 2016). In 2010, when the last census was made, more than 53 million people lived there, with a population density of approximately 34 inhabitants per km^2 (IBGE, 2010).

Climatology and droughts The semiarid region of NEB has a history in drought events, with reported data since the sixteenth century (Marengo et al., 2016). Between middle 1990s and 2016, 16 out of 25 years showed rainfall below normal in the region, and between 2010 and 2017 the most severe drought ever

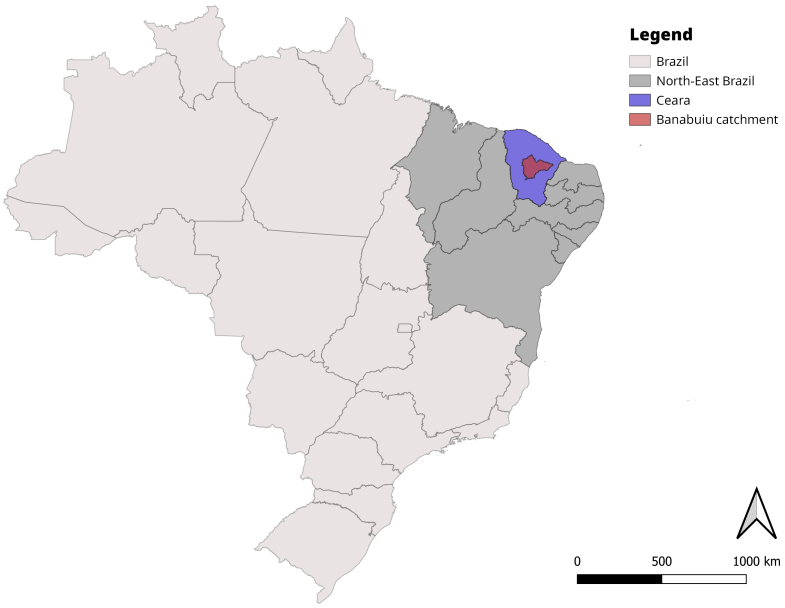

Figure 1.1: *Study area framing: North-East Brazil, Ceará and Banabuiú catchment*

recorded happened (Marengo et al., 2018). Climate projections show a rise in temperatures and rainfall reductions, and the tendency for increases in Consecutive Dry Days (CCD) suggests an increase in frequency and intensity of dry spells and droughts leading to aridification in the region (Marengo et al., 2016).

1.1.2 Banabuiú river basin

The Banabuiú basin is a watershed located in the NEB, in the State of Ceará. It is itself a sub-catchment of the Jaguaribe river basin and it covers an area of approximately 19,530 km^2, comprising 31 municipalities with approximately 914,000 inhabitants (IBGE, 2010).

Morphology The elevation in the basin ranges from mountain areas around 1100 m above sea level (ASL), in the eastern part, to mostly flat areas below 100 m towards the western part, as shown in Figure 1.2b. The main river in the basin is Rio Banabuiú, followed by its main tributary Rio Quixeramobim. The river network delineates the division of the basin into sub-basins, which are shown in Figure 1.2a with the associated code that will be used in the following Chapters.

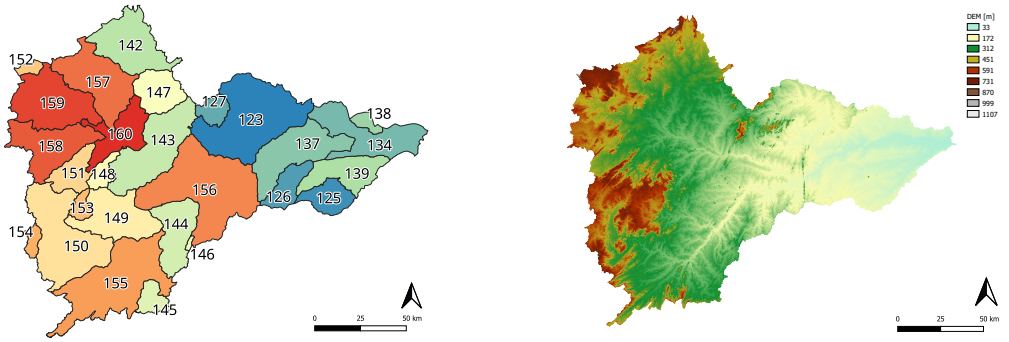

(a) *Sub-basins delimitation*

(b) *Digital Elevation Model (DEM) based on NASA's SRTM 90m from CGIAR*

Figure 1.2: *Banabuiú basin morphology visualization*[1]

1.2 Problem statement

Water supply in NEB relies on the reservoirs that regularize discharges. Storage capacity varies from small reservoirs used on private properties (in this study, a reservoir is considered small when its capacity is lower or equal to 500,000 m^3) to large reservoirs used for urban supply, industrial demands and large irrigation areas (also called hydrosystems). This system has a cumulative capacity of 707.36 billion m^3, according to the database from Reservoir Monitoring System of the Brazilian National Water Agency (Agência Nacional de Águas e Saneamento Básico (ANA)) in 2016. The NEB has a total of 17,083 reservoirs with surface area greater than 5 ha (Nascimento and Ribeiro Neto, 2017). Smaller reservoirs are built in dryland regions both as a drought preparedness measure and to respond to the growing water demand (Rabelo et al., 2021). In the Ceará state alone, a recent survey found a total of 105,813 existing reservoirs (FUNCEME et al., 2021). The Banabuiú river basin makes no exception, with a cumulative 2.1 $\cdot 10^8 m^3$ of capacity retained in 10,355 small reservoirs[2]. These reservoirs constitute the DRN, whose classification is reported in Table 1.1. The centralized reservoirs present in the basin, listed in Table 1.2 and visualized in their locations in Figure 1.3, account for a total capacity of 2.79 billion of m^3, the 92.91% of the overall total capacity.

Despite their small proportion in relation to total capacity (7.1%), small and medium reservoirs have an important role in the water supply of small rural communities whose needs are not met by the large hydrosystems, as the water stored in the small reservoirs enables local distribution. However, small reservoirs can reduce the potential yield of large, centralized reservoirs, which may

[1]CGIAR website: `https://srtm.csi.cgiar.org/`
[2]Results obtained from the processing described in Section 3.2.3

Table 1.1: *DRN's reservoirs classification in Banabuiú's basin*

Class	Upper bound m^3	Reservoir count	% over the total count	Class capacity m^3	% over the total capacity
1	5000	6977	67.4	$7.2 \cdot 10^6$	3.4
2	25000	1787	17.3	$2.1 \cdot 10^7$	10.0
3	50000	546	5.3	$2.0 \cdot 10^7$	9.4
4	100000	447	4.3	$3.2 \cdot 10^7$	14.8
5	500621	598	5.8	$1.3 \cdot 10^8$	62.4
Total	-	10355	100	$2.1 \cdot 10^8$	100

Table 1.2: *Banabuiú catchment centralized reservoirs information*

Name	Year constructed	Maximum capacity m^3	Drainage area km^2	ID code
Arrojado Lisboa	1966	$1.6 \cdot 10^9$	14.221	156
Capitão Mor	1988	$6 \cdot 10^6$	110	154
Cedro	1906	$1.26 \cdot 10^8$	206	127
Cipoada	1992	$8.61 \cdot 10^7$	351	126
Curral Velho	2007	$1.22 \cdot 10^7$	79	138
Fogareiro	1996	$1.19 \cdot 10^8$	5.111	160
Jatobá	1997	$1.07 \cdot 10^6$	40	146
Monsenhor Tabosa	1998	$1.21 \cdot 10^7$	77	152
Patu	1988	$7.18 \cdot 10^7$	995	149
Pedras Brancas	1978	$4.34 \cdot 10^8$	1.937	123
Pirabibu	2000	$7.4 \cdot 10^7$	503	147
Poço do Barro	1988	$5.2 \cdot 10^7$	374	125
Quixeramobim	1966	$7.88 \cdot 10^6$	7.021	143
Sao José I	1988	$7.67 \cdot 10^6$	188	148
Sao Jose II	1992	$2.91 \cdot 10^7$	185	145
Serafim Dias	1995	$4.3 \cdot 10^7$	1.63	150
Trapiá II	1992	$1.82 \cdot 10^7$	129	153
Umari	2011	$3 \cdot 10^7$	975	142
Vieirão	1988	$2.1 \cdot 10^7$	400	151

determine a lower possibility to store and distribute water during droughts (Krol et al., 2011). It is thus relevant to understand the hydrological impact of this dense network of (small) reservoirs (Ribeiro Neto et al., 2021).

As proposed by (Gutiérrez et al., 2014), articulating the role of drought preparedness in the context of watershed management areas with long term view can be an important practice to mitigate drought effects in Northeast Brazil. This implies also the recognition and consideration of the small reservoirs network throughout all the regions. Reservoir construction has been identified as capable to generate an higher water demand, and at the same time reducing the incentive for adaptive actions on other levels (Di Baldassarre et al., 2018).

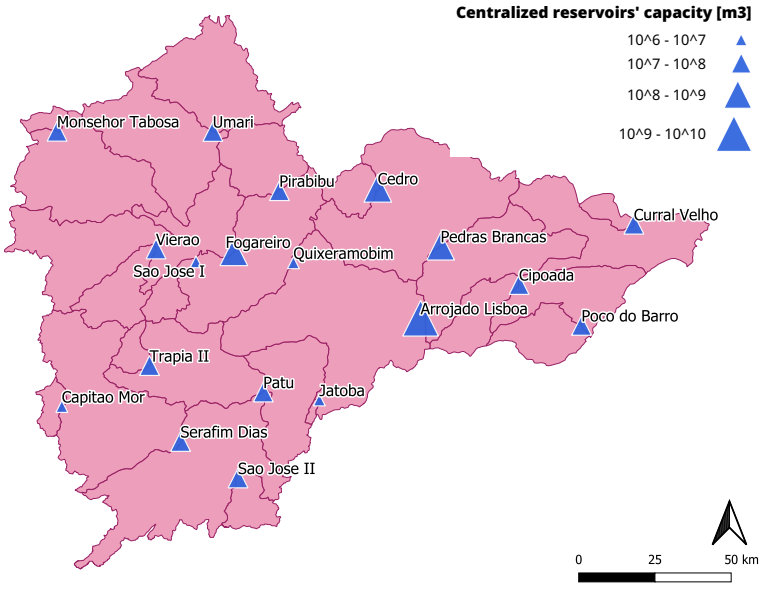

Figure 1.3: *Positions and capacities of the centralized reservoirs in the Banabuiú basin*

Cooperation between the operators of small and centralized reservoirs is also a possibility to evaluate, and it will be discussed in Section 5.3.

The aim of this thesis is thus to evaluate the influence of the DRN on drought evolution in the Banabuiú Basin, in the State of Ceará, North-East Brazil, considering also its impact on water availability throughout the considered region. This study contributes to the realization of 3DDD: Diagnosing drought for dealing with drought in 3D[3], a 4-year international project aimed to create a toolbox for increasing drought preparedness of actors in water and climate governance, starting from northeastern Brazil. This thesis assesses the second D: socio-hydrological simulation as a tool to analyze drought impacts due to human action.

[3]Project's website: `https://3ddd-project.org/`

2

Objectives and research questions

2.1 Objectives

This thesis focuses on two main objectives:

- Establish the role of the dense network of small water reservoirs (DRN) in the evolution of hydrological droughts in the Banabuiú basin, in the state of Ceará, North-East Brazil, by analyzing the past 40 years of precipitation and hydrological data and utilizing an hydrological model to reproduce and simulate the area in different conditions.
- Evaluate the effects of the existence of the DRN in time and space on the drought cycle (meteorological, hydro-meteorological, hydrological and no drought), and their role in shifting the equilibrium from a centralized condition of water resources to a distributed one.

2.2 Research questions

The objectives translates into the main research question of the study:
Which have been the effects in time and space of the existence of a dense reservoir network on the hydrological drought evolution in the past 40 years in the Banabuiú basin, in North-East Brazil?

The main question can be articulated into the following sub-questions:

- How can a dense network of small reservoirs be modeled effectively in a complex basin?

- How did the existence of a DRN influence the evolution and the intensity of drought periods in the past 40 years?
- How does the existence of a DRN influence the distribution of water resources across a river basin?

3

Methodology

After having defined the research questions, the approach to find answers to them was developed. These have been identified in the Drought Cycle Analysis (Ribeiro Neto et al., 2021) to address the DRN's effects on time and in the Downstreamness analysis (van Oel et al., 2018, 2011) to address the effects in space. They will be explained in detail in Chapter 3.4. These analyses have been carried out on two different scenarios: a scenario representing the reality, where the dense network of reservoirs exists, and a fictional scenario where it is not present anymore. A semi-distributed hydrological model was applied to simulate them, which takes the distribution of small reservoirs over the landscape into account, since the real-world observations alone are not enough to deal with this issue. The WASA-SED model (Water Availability in Semi-Arid environments-SEDiments) has been selected for this purpose, being able to model wide semi-arid areas considering both state-controlled centralized reservoirs and networks of diffused reservoirs (Güntner, 2002; Güntner et al., 2004; Mueller et al., 2010). This Chapter describes the data collection (Section 3.1), the data processing (Section 3.2), the model and the operations needed to apply it to the study area (Section 3.3) and the analysis performed (Section 3.4).

3.1 Data collection

The first necessary step was the data collection. The necessary data for running the model and performing the analysis is divided in:

– Meteorological data: temperature, precipitation, humidity, radiation

- Hydrological data: centralized reservoirs volume and release time series
- DRN data: location of the small reservoirs

The analysis time period takes place from 1980 to 2018, so the data have been collected for this period.
Below are listed sources and other information about the data collected.

3.1.1 Meteorological data

The meteorological data was obtained thanks to Fundação Cearense de Meteorologia e Recursos Hídricos (FUNCEME), Ceará's research institute for meteorology, water resources and environment. They manage a rainfall monitoring system with 550 conventional rainfall stations and general meteorological stations throughout the whole State of Ceará. The data collected contained information gathered by all the stations throughout the State. These observations have been used for both the modeled scenarios simulations and the subsequent Drought Cycle Analysis. In Table 3.1, the different data is listed with its source and the range of time in which they were available. INMET refers to Instituto National de Meteorologia, Brazil's national meteorological institute, of which FUNCEME has access to the meteorological time series as well.

Table 3.1: *Meteorological data information*

Data	Source	Overall availability	Temporal resolution	Number of stations
Precipitation	FUNCEME	1980-2018	daily	744
Temperature	FUNCEME	2005-2018	daily	90
Humidity	FUNCEME	2010-2018	daily	83
Radiation	INMET	2010-2018	daily	14

Insert image with the stations distribution in Ceará state
Also highlight the Banabuiu area

Temperature, humidity and radiation data didn't cover all the time period from 1980 to 2018, so synthetic data already used in literature in the same study area has been used (Mamede et al., 2018).

3.1.2 Hydrological data

The hydrological data of the centralized, state-controlled reservoirs was obtained thanks to FUNCEME, which has access to this information in the State of Ceará. The observations of the reservoirs' volumes have been used to calibrate and validate the WASA-SED model, while the observations of their releases have been used as a valuable input to the model.

The centralized reservoirs in the study area (Banabuiú's river catchment) are listed in Table 1.2, with their maximum capacity and their identification code of the sub-catchment in which they are located. The latter will be used in the following chapters and can be spatially visualized in Figure 1.2. The gathered data information is found in Table 3.2.

Table 3.2: *Hidrological data information*

Data	Source	Availability	Temporal resolution
Centralized reservoirs' volumes	FUNCEME	1986-2018	daily
Centralized reservoirs' releases	FUNCEME	1986-2018	daily

3.1.3 Location of the reservoirs forming the DRN

The location of the small reservoirs forming the DRN in the Banabuiú basin were obtained thanks to the mapping operated by FUNCEME for the Government of the State of Ceará in February 2021 (FUNCEME et al., 2021). In all of Ceará State, the reservoirs were identified starting from satellite images. Then, geo-processing operations were applied to improve the result an integrate them with cadastral information. The total mapped reservoirs by this study in the Ceará State are 105,813, of which 17,299 (16%) are located in the Banabuiú basin. This data didn't contain information about the reservoirs' areas nor volume, so this information had to be obtained as explained in Section 3.2.3. The visual representation of DRN's distribution over the basin (after being processed) is shown in Figure 3.2.

3.2 Data processing

The gathered data needed to be processed in order to be used both as input to the model and for the subsequent analysis. Basic pre-processing operations have been used on the data to have a reliable and effective dataset: identification of anomalous stations, outlier rejection, missing values handling. To obtain the meteorological data in each of the sub-catchments composing Banabuiú's basin, an interpolation based on Thiessen polygons was operated on the whole dataset of stations available. The reservoirs included in the DRN needed to be associated with their surface covered to be able to express them in terms of volume through an area-volume relationship, and this has been done using JRC's Global Surface Water Explorer. All the data handling has been performed through R[1], while some of DRN's handling operations have been performed on

[1] R version 4.0.1. Website: `https://www.r-project.org/`

QGIS[2].

3.2.1 Meteorological and hydrological data pre-processing

The meteorological and hydrological data here discussed refer to Tables 3.1, 3.2, respectively. The pre-processing of the meteorological data focused on removing anomalous monitoring stations, removing eventual outliers in the time series and handling the missing data. The hydrological data were instead already pre-processed time series, so no pre-processing operations were performed on them. Thus, the description of the operations below will only refer to meteorological data. In the last paragraph an anomaly found in one reservoir volume's time series will be discussed.

Anomalous stations removal The criteria used to define an "*anomalous*" station in the available dataset was to check if it had repeated negative values registered. This assumption was made considering that no meteorological variable could have negative values registered (aside from temperature, where this method wasn't used), so a station which would present this negative anomaly had encountered some instrumental failure, and thus was removed as not reliable. In total as a result of this method, 7 precipitation stations (out of 744) and 1 radiation station (out of 14) have been removed from the dataset.

Outlier rejection The Inter-Quantile Range (IQR) method was used to check and remove outliers from the dataset, a very well known and diffused technique (Rousseeuw and Hubert, 2011, 2018) based on the identification of occurrences outside a range of statistically-feasible values. As Rousseeuw and Hubert (2011) point out, this method is not accurate for skewed distributions, as it will flag many regular data points as outlying. Thus, for precipitation (a classic skewed-distributed variable), another method was used to identify the outliers. Many different precipitation outlier detection methods exist and have been tested and proposed (Wu et al., 2010; Mirzaei et al., 2014; Zhao and Yang, 2019). Here, an analysis on time series maxima and a literature review were performed to define a threshold above which an observation can be considered as an outlier. In Rodrigues et al. (2020), an approximated estimation of a daily precipitation with a return period of 100 years is set at 250 mm, so this value has been set as the threshold for identifying outliers: singular observations above this threshold have been replaced as missing values, and stations with exceptionally high values (in 10^3 order) were directly removed from the dataset, considering them

[2]QGIS version 3.10.6. Website: `https://www.qgis.org/`

not reliable. Nine precipitation stations over 737 have been removed with this method, confirming the anomalous nature of their observations, also comparing it with studies dated before the time series starting year (Ramos, 1975).

Missing values handling Missing values, both pre-existent and generated by the outlier rejection phase, were handled with a moving average algorithm included in R's *imputeTS* package specifically optimized to handle time series (Moritz, 2021).

Anomaly in the volume time series The collected Curral Velho's volume time series showed an anomalous behavior, more similar to a river flow dynamic than a reservoir's volume dynamic. Thus, Curral Velho reservoir has not been used in the model calibration phase, and the results of the analysis regarding it have to be labeled as not completely reliable results since this reservoir has not been calibrated.

3.2.2 Interpolation of meteorological data

To obtain the meteorological data for each sub-basin in the Banabuiú basin, an interpolation using the dataset available has been carried out. The selected Thiessen polygons method was selected to perform this operation, due to its easy implementation and its consolidated utilization in previous studies, but numerous other methods have been used in the literature, sometimes highlighting the lack of flexibility of the Thiessen polygons method (Sen, 1998). The main concept of this method is to construct a geo-referenced layer of Thiessen polygons (also known as Voronoi polygons or Voronoi diagrams) around the meteorological stations locations: they define an area around a point (the station) where every location is closer to this point than to all the others. This structure is then overlaid on the sub-basins layer, which contains the area information of each sub-basin, as in Figure 3.1. The n overlapping areas of polygons over each sub-basin are then used as weights (W_i) to multiply the meteorological variable's value corresponding to that polygon, in order to compute its weighted mean (v^{sub}_{Wmean}) and assign it to the sub-basin, as

$$v^{sub}_{Wmean} = \frac{\sum_{i=1}^{n} W_i \cdot v_i}{\sum_{i=1}^{n} W_i}$$

. Since the number of available stations changed through time, an automatic and daily based approach was used, computing the Thiessen polygons and the weighted mean for each day of the available dataset. The final output of

the method is then a simple dataframe with dates as rows and the sub-basins as columns, with the cells containing the weighted average of the meteorological value. All these procedures were performed through *R*, using functions from *deldir*, *raster* and *rgdal* packages (Turner, 2021; Hijmans, 2021; Bivand et al., 2021).

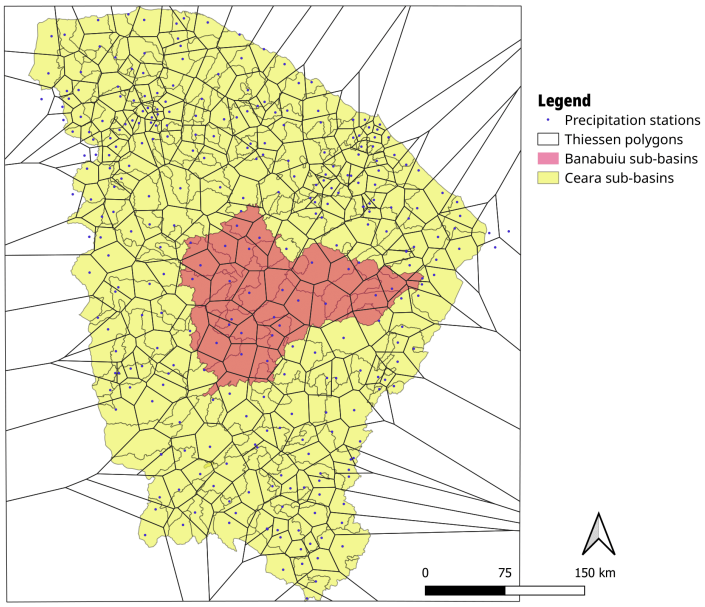

Figure 3.1: *Example of the Thiessen polygons computed on precipitation stations' location at a random date (01-01-2000)*

3.2.3 DRN capacities estimation

The DRN locations illustrated in Section 3.1.3 did not contain information about the surface area nor the capacity of the reservoirs. Therefore, the capacity information, needed to represent the network in the hydrological model and the subsequent analysis, has been obtained starting from JRC's Global Surface Water Explorer[3], which provides a worldwide database of surface water imagery (Pekel et al., 2016). The maximum water extent raster[4], which maps the maximum extent of water bodies in an area, was downloaded for the Banabuiú basin. It was then processed by vectorializing it (obtaining polygons out of groups of pixels, through *QGIS* tools), then removing the polygons corresponding to the centralized reservoirs and polygons labeled as not representing water bodies (through *R*). The result was then connected with the original locations of the DRN, by associating each reservoir location to the nearest water body

[3]JRC's Global Surface Explorer website: `https://global-surface-water.appspot.com/`
[4]Raster: matrix data structure that represents a rectangular grid of pixels

through a Nearest Neighbor approach, performed through the *NNJoin* plugin in *QGIS*[5]. In this way, in the joined output, each reservoir had an associated area. Some reservoirs didn't have a correspondent water body in the JRC's representation, probably due to their small size, which is difficult to be detected and validated through satellite images, or due to errors in the survey operated by FUNCEME et al. (2021), where small depressions (e.g. roads) could have been interpreted as reservoirs. These reservoirs were left out of the final configuration, since in the first case their capacity should have been estimated in a different way, losing coherence, and in the second case wrong data would have been considered. Approximately 7,000 small reservoirs were left out, resulting in 10,355 small reservoirs with their maximum area associated. The capacity of each reservoir (V) was obtained from the area (A) through Molle's equation (3.1), where α and K parameters are equal to average values of 2.7 and 1,500 respectively, as used in literature in North-East Brazil (Mamede et al., 2018, 2012). Table 1.1 was obtained thanks to the result of this procedure, and the final DRN distribution is shown in Figure 3.2.

$$V = K \cdot \left(\frac{A}{\alpha \cdot K}\right)^{\frac{\alpha}{\alpha - 1}} \tag{3.1}$$

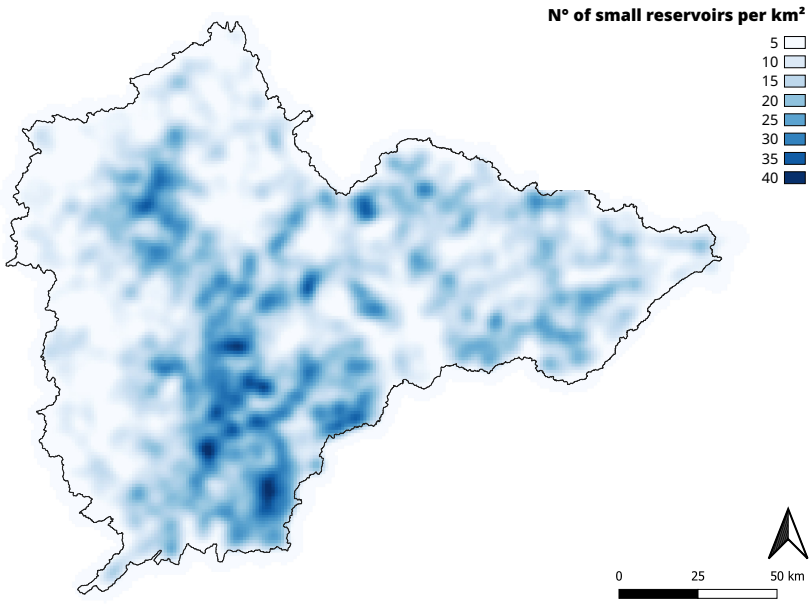

Figure 3.2: *DRN's density visualization in the Banabuiú basin*

[5]NNJoin plugin website: `https://plugins.qgis.org/plugins/NNJoin/`

3.3 Modeling

To produce the necessary scenarios for the subsequent analysis, an hydrological model had to be used to simulate the system under the premises of both scenarios: the existence and the non-existence of the DRN. The model selected is WASA-SED, which has been developed and utilized to simulate North-East Brazil's conditions (Güntner, 2002; Güntner et al., 2004; Mueller et al., 2010). In this section the modeling approach will be briefly explained, as well as the process towards the final model's outputs.

3.3.1 WASA-SED model

The WASA-SED model (Water Availability in Semi-Arid environments-SEDiments) simulates the runoff and erosion processes at meso-scale, for domains ranging from several hundreds to thousands of square kilometers. It uses a hierarchical top-down disaggregation scheme, dividing each sub-basin of the model into landscape units (based on the Soil and Terrain Digital Database (SOTER) concept (Oldeman and van Engelen, 1993)), represented by multiple terrain components (defined by slope-gradient, length, soil and soil-vegetation components). Within and between terrain components, the vertical fluxes for typical soil profiles are taken into account (Mueller et al., 2010). The hydrological module is fully described in Güntner (2002) and Güntner et al. (2004), implementing for example equations to account for interception losses, evaporation and transpiration (modified Penman-Monteith approach (Shuttleworth and Wallace, 1985)) and for infiltration (Green-Ampt approach (Green and Ampt, 1911)) and other soil and vegetation related processes. The model can simulate both large centralized reservoirs and small diffuse networks of reservoirs (Güntner et al., 2004). The WASA-SED model was developed within the joint Spanish-Brazilian-German research project SESAM (Sediment Export from Semi-Arid Catchments: Measurement and Modelling). The model is coded in Fortran90 language; the user manual, the link to the source code and other useful sources can be found at Güntner et al. (2021).

Reservoirs module The modeling approach to the reservoirs needs to classify them into strategic and small reservoirs, according to location and size. Strategic reservoirs are medium and large sized reservoirs (with storage capacity higher than $10^6 m^3$ in the presented configuration) located on main rivers at the sub-basin's outlet, while small reservoirs are distributed throughout the sub-basin area. The strategic reservoirs are characterized in-depth, as explained in

Section 3.3.2. Since the uncontrolled and unmonitored nature of these small reservoirs, not enough information is available concerning dam building, location, size and water use, so the model represents them in a simplified manner based on a classification and grouping into size classes according to storage capacity (Güntner et al., 2004; Mamede et al., 2018). Water routing is performed for each sub-basin using a cascade routing scheme (Figure 3.3). The generated runoff within the sub-basin is distributed among the reservoir classes using a weighting factor computed as a ratio between the runoff contributing area of that reservoir class and the sub-basin area. The original cascade routing scheme developed by Güntner et al. (2004) assumes that generated runoff within the sub-basin is distributed equally to each reservoir class. The water balance is computed for one hypothetical *representative* reservoir with mean characteristics, obtained considering the storage capacities of all reservoirs in each class and sub-basin, and the water storage volume V_r of each class r of small reservoirs is obtained through Equation 3.2. Strategic reservoirs' water balance is instead calculated explicitly and individually for each reservoir, considering also the operation rules given as input. A detailed description of the calculation of water fluxes through the classes of reservoirs can be found in Mamede (2008), while equations and other information about the hydrological and reservoir module can be found in Güntner (2002).

$$V_{rm} = V_{o,rm} + \frac{Q_{in,r} - U_r}{n} - Q_{out,rm} + (P_{rm} - E_{rm}) \cdot A_{rm} - I_{rm}$$
$$V_r = n \cdot V_{rm} \tag{3.2}$$

where:

V_{rm} = water storage of the class' representative reservoir rm (m^3);
$V_{o,rm}$ = V_{rm} at the beginning of the time step (m^3);
$Q_{in,r}$ = water inflow to reservoirs of class r within the time step (m^3);
U_r = water withdrawal from class r (m^3);
P_{rm} = precipitation falling directly onto the reservoir surface (m);
E_{rm} = evaporation form the reservoir surface (m);
A_{rm} = surface area of the reservoir rm (m^2);
I_{rm} = infiltration loss to alluvium and bedrock (m^3).

3.3.2 Model inputs and parameterization

The Banabuiú basin was divided into the 21 sub-basins shown in Figure 1.2 (a). Each sub-basin's landscape, terrain units, soil-vegetation components and soil profiles were already parameterized from previous studies (Souza et al., 2013).

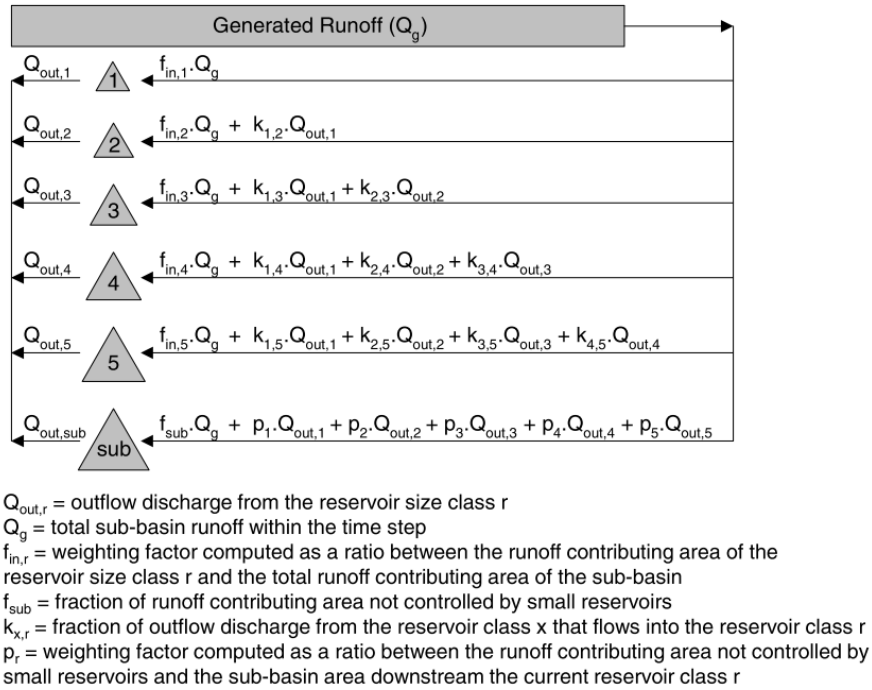

Figure 3.3: *Cascade routing scheme through the reservoir size classes, taken from Mamede et al. (2018)*

The meteorological data needed as input was obtained through the interpolation explained in Section 3.2.2. The reservoirs' release time series were used in the model for reservoir water abstraction.

Strategic reservoirs parameterization

Morada Nova and Umari reservoirs were missing from the parameterization available from previous studies, because they were built after the parameterization was made. Their parameters had then to be obtained to be able to simulate them with WASA-SED. The necessary parameters for both reservoirs are listed in Table 3.3. They were filled in the input file *reservoir.dat*. Aside from those reported there, the area-volume relationship points were added to the input file *cav.dat* (both files are explained in Güntner et al. (2021)). The parameters were obtained from COGERH and FUNCEME databases for the corresponding reservoirs (COGERH et al.; FUNCEME). *dama* and *damb* parameters are respectively the a and b parameters of the Area-Volume relationship:

$$A = a \cdot V^b$$

. They were derived from Molle's equation (3.1) parameters α and K (Molle, 1994), through a linear regression as instructed in Molle (1994), pag. 20, then

obtained as:

$$a = (\frac{1}{K} \cdot \alpha K^{\frac{\alpha}{\alpha-1}})^{\frac{\alpha-1}{\alpha}}$$

$$b = \frac{\alpha - 1}{\alpha}$$

. *damc* and *damd* parameters are respectively the c and d parameters of the spillway rating curve:

$$Q = c \cdot H^d$$

where H is the water height over the spillway and Q is the overflow discharge.

Table 3.3: *Parameters assigned to Morada Nova and Umari reservoirs*

	Reservoirs	
Parameter	**Morada Nova**	**Umari**
Sub-basin ID	138	142
Initial minimum level [m]	75	294
Maximum level [m]	84.6	310
Initial volume [$1000 \cdot m^3$]	unknown	unknown
Initial storage capacity [$1000 \cdot m^3$]	12,165.745	30,000
Target release through the the intake devices [m^3/s]	0.401	0.39
Maximum fraction of dam flow released	0.9	0.9
Water withdrawal to supply the water use sector* [m^3/s]	0.183	0.229
Year of construction	2007	2010
Initial maximum area [*ha*]	413	738.28
Initial dead volume [$1000 \cdot m^3$]	1,216.57	3,000
Initial alert volume [$1000 \cdot m^3$]	1,216.57	3,000
dama	57.5	11.883
damb	0.68	0.787
damc	80	96
damd	1.5	1.5

* Indicative value (equal to the Q90), the actual withdrawal will be computed through the intake release time series.

DRN parameterization

The DRN obtained from Section 3.2.3 was divided into 5 classes, the same used to obtain Table 1.1, and for each sub-basin the reservoirs contained in each class were computed and assigned. The final classification used to reproduce the scenarios including the DRN is shown in Table B.2. Here an approximation is introduced: the amount of small reservoirs considered for each year remains the same as the starting point obtained from Section 3.2.3. This was necessary because the survey from which the reservoirs locations and volumes were derived was made in 2020 (FUNCEME et al., 2021). Moreover, approximately 7 thousands small reservoirs were removed by precaution in the processing phase, equal to the 40% of all the reservoirs surveyed.

3.3.3 Calibration

From previous studies and experience in the calibration of WASA-SED model (Güntner, 2002; Mamede et al., 2018), this is mainly focused on changing one parameter for each sub-basin, a scaling factor to modify the hydraulic conductivity during infiltration: all values for saturated hydraulic conductivity during infiltration in the sub-basin are divided by its corresponding scaling factor (Güntner et al., 2021). The calibration was then carried out automatically following the sub-basins routing path of the model (shown in Figure 3.4), from upstream to downstream. One sub-basin at a time, the scaling factor was increased from 0.2 to 7 with a step of 0.2. For each run, five indexes were computed (R^2, NSE, KGE, PBIAS and NRMSE)[6] comparing the modeled volume time series for the sub-basin's reservoir (or the direct downstream one in case the sub-basin didn't present one itself) with the observed one. The indexes were selected based on previous usage in this field (Marahatta et al., 2021; Knoben et al., 2019; Uniyal et al., 2019). The selected parameter for each sub-basin was identified as the one who would produce the best performance in the indexes for the considered sub-basin's reservoir.

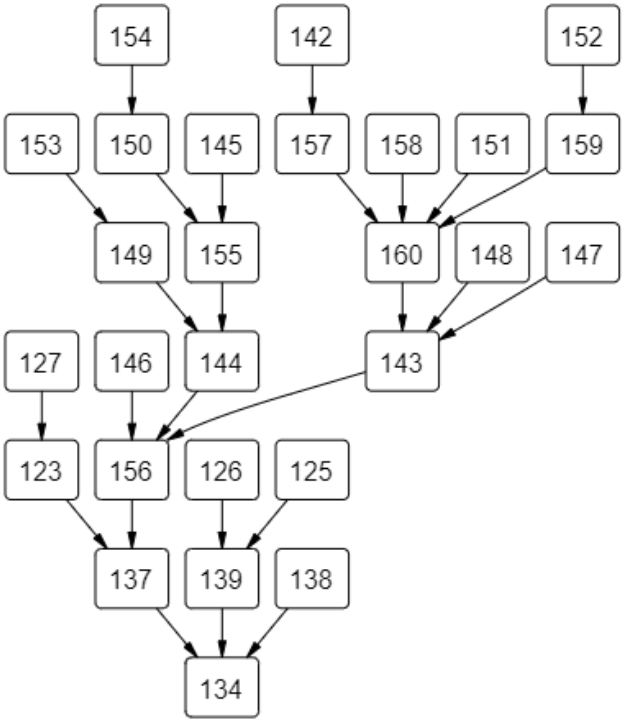

Figure 3.4: *Sub-basins routing scheme in the Banabuiú basin followed by the model and in calibration*

[6] R^2: Coefficient of determination; NSE: Nash-Sutcliffe Efficiency; KGE: Kling-Gupta Efficiency; PBIAS: Percentage of Bias; NRMSE: Normalized Root Mean Squared Error

The uncalibrated model version was obtained by running the model with all the scaling factors equal to 1, meaning no calibration of the hydraulic conductivity. This configuration was used to compare the calibrated model results both numerically and visually, as in Figure 3.5.

Validation

The calibration was performed on the 70% of the series, running the model between 1980 and 2006 (27 years), then the model was validated running it with the calibrated set of parameters on the remaining 30% of the series, from 2007 to 2018 (12 years). Approximately 945 runs were performed and evaluated. In Table 3.4 the calibration, validation and whole time series mean performances over the sub-basins are shown for each index, while the single sub-basins performances are shown in Table B.3. As stated by Klemeš (1986) in his explanation of the *Split-sample test*, "the model should be judged acceptable only if the two results are similar and the errors in both runs are acceptable". The results are similar in both runs and also in the whole time period, and the performances are considerable as acceptable: the parameterization is kept, and the single values of the scaling factors are shown in Table B.1.

Table 3.4: *Mean performance of WASA-SED model after calibration, validation and on the whole time series*

Index	**Calibration period** (1980 − 2006)	**Validation period** (2007 − 2018)	**Whole period** (1980 − 2018)
R^2	0.598	0.600	0.519
NSE	0.0497	0.360	0.271
PBIAS	7.853	-3.881	-1.523
KGE	0.462	0.572	0.674
NRMSE	0.257	0.239	0.246

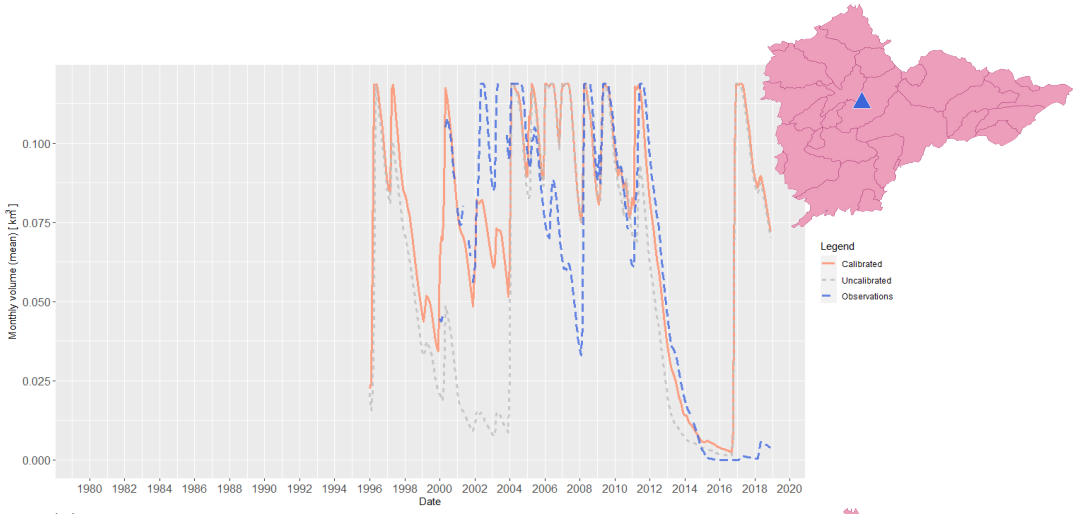

(a) *Fogareiro*

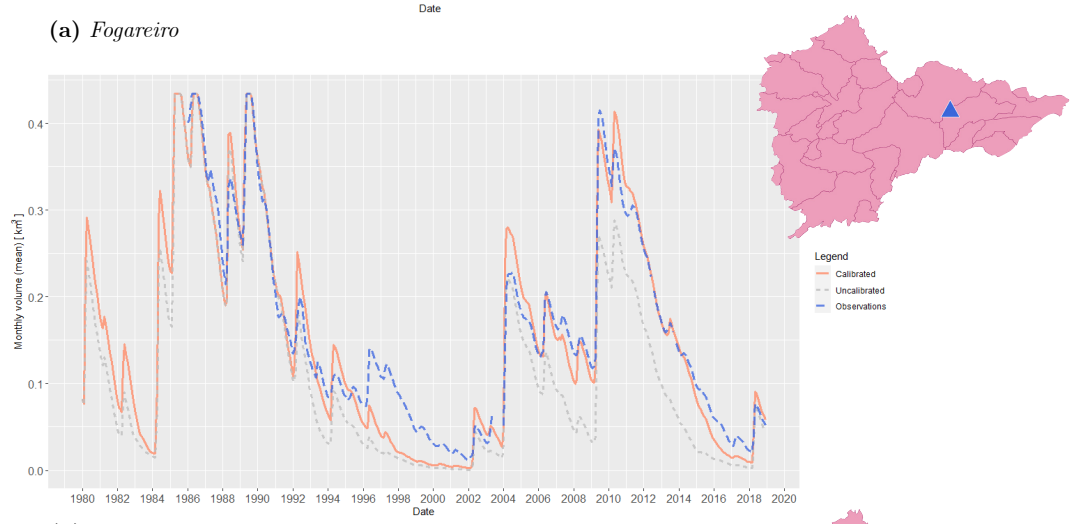

(b) *Pedras Brancas*

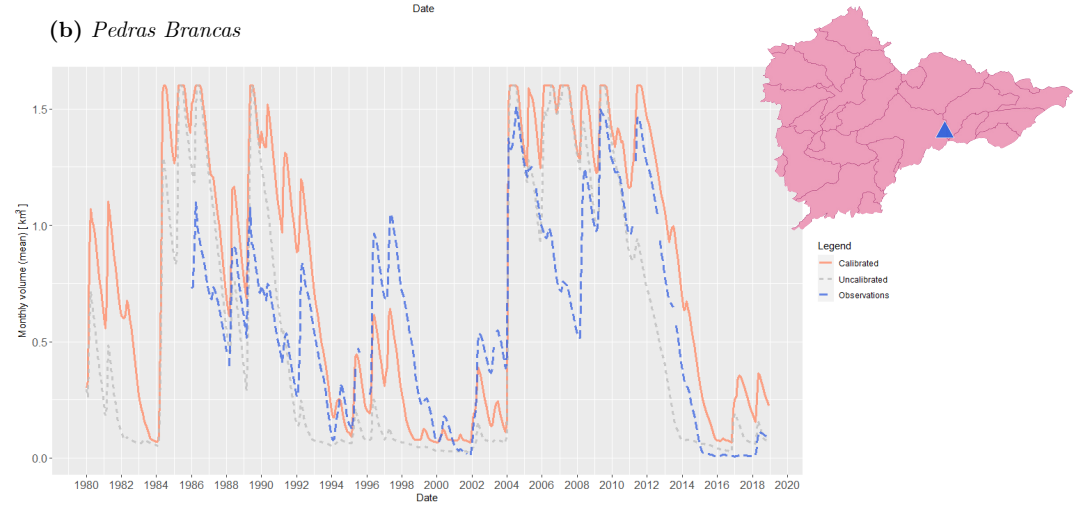

(c) *Arrojado Lisboa*

Figure 3.5: *Pedras Brancas, Arrojado Lisboa and Fogareiro reservoirs modelled volumes after calibration, compared with uncalibrated and observations*

3.3.4 Generated scenarios

The last step was the generation of the two scenarios needed to perform the analysis. The first scenario, named *All Reservoirs (AR)*, was obtained by running the model in the same configuration obtained after the calibration over the $1980 - 2018$ period, so including the network of small reservoirs parameterized as in Section 3.3.2. The second scenario, named *Large Reservoirs (LR)*, was obtained by running the model removing the small reservoirs network, by giving the model a blank parameterization file for the network (*lake_ number.dat*). In order to further explore the effects of the DRN, two additional scenarios are simulated. These scenarios are modeled by including in the Water Availability in Semi-Arid environments-SEDiments (WASA-SED) model only reservoir Arrojado Lisboa as centralized reservoir, and consider one configuration with the DRN present (*Small Reservoirs (SR)*) and one without it (*Naturalized (N)*). This design permits to remove the effect of the other centralized reservoirs, focusing on the role of the DRN in Arrojado Lisboa's volume variations without their influence. The four modeled scenarios design is visualized in Figure 4.1.

3.4 Analysis

To effectively consider the effects that the existence of an DRN produces on drought evolution, two domains have been considered: time and space. At a first thought, in the time domain, the presence of this network will influence the persistence and frequency of the hydrological droughts on the centralized reservoirs, and at the same time, in the spatial domain, they will permit a broader and more diffuse water availability throughout the basin. This dual aspect has to be considered when assessing the effects of the network, and the validity of the previous consideration will be assessed by the analysis' results in Chapter 4. In the following sections, the two analysis performed to be able to explore the effects in the two domains are explained:

- Effects in time: Drought Cycle Analysis, Section 3.4.1
- Effects in space: Downstreamness analysis, Section 3.4.2

Both the analysis will be performed comparing the AR and LR modeled scenarios obtained as in Section 3.3.4.

3.4.1 Effects in time: Drought Cycle Analysis

The Drought Cycle Analysis (DCA) is a recent method proposed by (Ribeiro Neto et al., 2021), based on a combination of precipitation and hydrological

Table 3.5: *Drought cycle phases related to PI and WSI indexes' values*

Stage	PI range	WSI range
1. Non-occurence of drought	> 0	> 0
2. Meteorological drought	< 0	> 0
3. Hydro-meteorological drought	< 0	< 0
4. Hydrological drought	> 0	< 0

indexes to classify a region's conditions through time into four possible stages:

1. Non-occurrence of drought

2. Meteorological drought: marks the onset of a precipitation deficit. Precipitation decreases and the region enters a dry period.

3. Hydro-meteorological drought: coexistence of meteorological and hydrological drought. The water storage is affected by the persistence of the meteorological drought, the reservoirs depletion cross a certain threshold.

4. Hydrological drought: persistence of hydrological impacts after the end of the meteorological drought. The reservoirs may start to recharge thanks to the end of the meteorological drought, but are still in a depletion condition.

In order to identify the stage of a region at a certain time, two indexes are considered: a Precipitation Index (PI) and a Water Scarcity Index (WSI), whose names are self-explanatory on their purpose, and exist in many different forms. For the purpose of this analysis, negative values of the index mean a scarcity condition, while positive values mean the opposite. In Table 3.5, the relationship between these indexes' values and the corresponding phase is highlighted.

The '*wheel*' used to represent these stages is shown in Figure 3.6. It has the structure of a Cartesian reference system, with the PI as y axis and the WSI as the x axis. When placed on the wheel, so, also the information about the magnitude of the phase is showed: the closer will be an event to the circumference, the higher will be its intensity.

In order to compute the analysis, the Precipitation Index and the Water Scarcity Index can be chosen from the many available. Here it has been followed the same procedure followed in (Ribeiro Neto et al., 2021), using the Standardized Precipitation Index (SPI) as a PI and the Volume Deviation (VD) as a WSI, which are both explained in the next paragraphs, but different studies and tools are available to select drought indicators (Zaniolo et al., 2018). The indexes are computed at monthly resolution, the results of the Drought Cycle Analysis will then have a monthly resolution themselves.

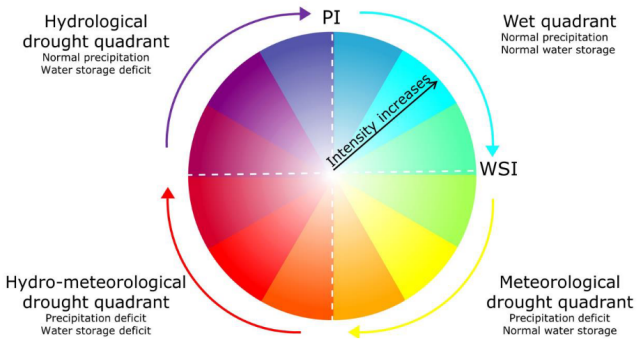

Figure 3.6: *Drought Cycle Analysis method graphical representation, from Ribeiro Neto et al. (2021)*

SPI computation The SPI is an index recommended by the World Meteorological Organization (WMO) and others in 2011 with the Lincoln Declaration of Drought Indices (Hayes et al., 2011), to standardizez the characterization of meteorological droughts around the world. Its value can range approximately form -2 to +2, but can also be higher or lower than these boundaries (WMO, 2012). As stated in WMO (2012), a drought event occurs any time the SPI is continuously negative and reaches an intensity of -1 or less. The event ends when the SPI becomes positive. Each drought event, therefore, has a duration defined by its beginning and end, and an intensity for each month that the event continues. Different time scales ranging from 3 to 48 months can be considered when computing the SPI, depending on the analysis' short or long term focus and also if other types of droughts needs to be investigated (e.g. agricultural). In this study, whose analysis are spanning through almost 40 years, the time scale selected was 12 months, the suggested time scale for hydrological analyses, with monthly results' time steps. The SPI was computed using the *SPEI* package in *R* (Beguería and Vicente-Serrano, 2017).
The index has been calculated on each sub-basin precipitation time series, then a broad result for the whole basin has been calculated through the mean. For the analysis, the SPI relative to Arrojado Lisboa's sub-basin has been considered. Since this index is only based on precipitation, it is good practice to associate it with other indexes when dealing with other types of droughts than just the meteorological one. The VD responds to this principle.

VD computation As proposed by Ribeiro Neto et al. (2021), the VD is an index considering the deviation of a reservoir's volume from the half of its total capacity, as showed in Equation 3.3. It can thus vary from -1 to 1, with positive values meaning a volume higher than half of the total capacity and negative values meaning the opposite.

$$VD_{i,r} = \frac{V_{i,r} - \frac{maxcap_r}{2}}{\frac{maxcap_r}{2}} \tag{3.3}$$

where:

$VD_{i,r}$ = Volume Deviation at month i, for reservoir r
$V_{i,r}$ = Volume at month i, for reservoir r
$maxcap_r$ = Maximum capacity of reservoir r

After regrouping the reservoirs' volumes into monthly steps, the VD was computed for all reservoirs. Then, a basin-representative value had to be chosen to perform the Drought Cycle Analysis. Reservoir Arrojado Lisboa's VD was selected for this task, since it is the most downstream centralized reservoir, collecting the above streams and outlets, thus able to represent the basin. Also the average of the VD of all the centralized reservoirs was considered for the task, but not selected due to the mean's mitigation effect on the values, leading towards more similar behaviors in the two modeled scenarios.

Effects evaluation By considering the SPI and the VD, we can determine if the area we are considering is in a drought condition and, if yes, in which of the three phases it is in. By considering two different scenarios (one including the DRN and one excluding it), we can evaluate the differences in drought cycles generated by the presence of the DRN, by comparing the persistence and frequency of drought phases. To compare drought events, each pair of observations is positioned into the corresponding quadrant of Figure 3.6's 'wheel', and differences in magnitude and drought phase are assessed.

3.4.2 Effects in space: Downstreamness analysis

The downstreamness concept is a method which aims to analyze the availability and distribution of water resources in a river basin, first introduced in van Oel (2009) and successively developed and used to analyze basin closure and to diagnose hydrological droughts (van Oel et al., 2011, 2018; van Langen et al., 2021). The downstreamness of a location (D_x), for example a reservoir's dam outlet, is the ratio of its upstream catchment area to the entire river basin area:

$$D_x = \frac{A_{up,x}}{A_{tot}} \cdot 100\%$$

. The downstreamness of a basin's function (like water availability or water demand) is defined as the downstreamness-weighted integral of that function divided by its regular integral (van Oel et al., 2011). In this study, the functions

considered are the basin's storage capacity and the basin's stored volume. In order to extract the upstream catchment area of the reservoirs (both DRN and centralized ones), a Digital Elevation Model (DEM) of the was downloaded through CGIAR' SRTM database (CIAT, 2021), then processed through *QGIS* tools to remove outliers and to obtain a flow accumulation raster, which contained the upstream catchment in each one of its pixel. The reservoirs point layers were then overlaid to this raster to extract their A_{up}, while the A_{tot} is taken at the basin outlet. The computation of D_x is then achievable. An assumption was made in order to be able to handle the DRN keeping their spatial information: the number of reservoirs was kept the same as the one obtained in Section 3.2.3 in the computation of the downstreamness, across all the years considered. This approximation means that considerations about the effects of the evolution of the DRN in time can not be made, but at the same time it makes the analysis on the effects more sound because it reduces the growing uncertainty about the number and location of small reservoirs in the past, since a mapping of the small reservoirs across the years in not available.

Downstreamness of Storage Capacity (D_{SC}) For analyzing the downstreamness of a basin's storage capacity, the capacity of reservoirs and the locations of dams are the key information. The downstreamness of the total storage capacity in a basin can change over time, due to newly built reservoirs or capacity loss by sedimentation. The storage capacities of the reservoirs are then used as weights to determine D_{SC}, which is a measure of how far downstream storage capacity in the basin is located on average (van Oel et al., 2011). For a basin with n reservoirs, D_{SC} is computed as

$$D_{SC} = \frac{\sum_{x=1}^{n} SC_x D_x}{\sum_{x=1}^{n} SC_x}$$

where D_x is the downstreamness of reservoir x and SC_x is its storage capacity (van Oel et al., 2011). In the analysis of this study, D_{SC} is computed for each year in the time period considered, in two scenarios: one including the DRN (*AR*) and one excluding it (*LR*).

Downstreamness of Stored Volume (D_{SV}) For analyzing the downstreamness of stored water volume in a basin, reservoir volumes and the locations of the dams are the key information. D_{SV} changes because volumes at different locations can change over time at different rates. The stored volumes at different time steps of the reservoirs are then used as weights to determine D_{SV}, which is a measure of how far downstream stored water in the basin is located on average (van Oel

et al., 2011). For a basin with n reservoirs, D_{SV} is computed as

$$D_{SV} = \frac{\sum_{x=1}^{n} SV_x D_x}{\sum_{x=1}^{n} SV_x}$$

where D_x is the downstreamness of reservoir x and SV_x is the stored volume in reservoir x. In the analysis of this study, D_{SV} is computed monthly for the time period considered for *AR* and *LR* scenarios computed as in Section 3.3.4. For the centralized reservoirs, this operation was straightforward once their D_x was determined and the reservoir's volume was obtained from the model. For the DRN, the WASA-SED model computes the small reservoirs volumes as 5 cumulative values for each of the 5 volume classes in each sub-basin (refer to Section 3.3). These values were divided by the number of small reservoirs in the respective sub-basin and class to obtain an average value; the average value was assigned to each reservoir of that sub-basin and class, as their SV_x. Once obtained each small reservoir's D_x, the D_{SV} could be computed.

Effects evaluation By considering the differences between the two scenarios in D_{SC} and D_{SV} it can be evaluated how the existence of the DRN influences the potential and actual water availability distribution in the region. The D_{SC} is then compared to the D_{SV} in order to obtain information about the allocation of water in the basin, showing whether more water is located upstream or downstream, or determine eventual filling rates discrepancies, as in Figure 3.7, where *(a)* depicts a situation with equal filling rates; *(b)* depicts a situation with an higher filling rate for the upstream reservoir and *(c)* a situation with an higher filling rate for the downstream reservoir. This means that if D_{SV} is lower than D_{SC}, more water is stored upstream, while the opposite means more water is stored downstream.

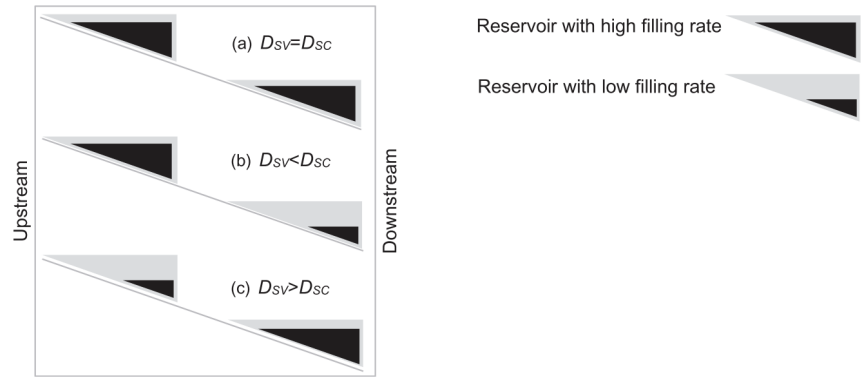

Figure 3.7: *Schematic depiction of three situations of reservoir filling rates for a river basin with two reservoirs, from van Oel et al. (2018)*

4

Results

In this Chapter the results of the performed analysis are shown: in Section 4.1 with the Drought Cycle Analysis, then Section 4.2 with the Downstreamness Analysis. A synthesis is presented in Section 4.3. The modeled scenarios, which were generated as explained in Section 3.3.4, are visualized in Figure 4.1 for better comprehension. The differences between *AR* and *LR* scenarios have been explored in order to assess the effects of the DRN on droughts' evolution in time and space. *N* and *SR* scenarios have been useful to explore the DRN effects without the influence of large reservoirs.

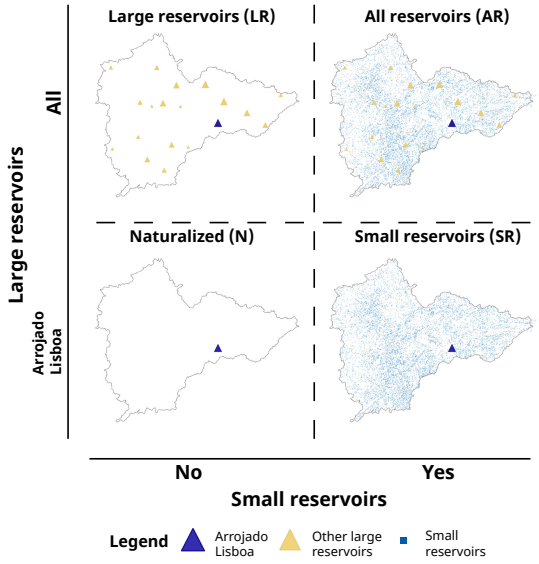

Figure 4.1: *Visualization of the modeled scenarios design: Large Reservoirs (LR), All Reservoirs (AR), Naturalized (N) and Small Reservoirs (SR)*

4.1 Drought Cycle Analysis outcomes

The results from the Drought Cycle Analysis are divided in three Sections, analysing the SPI and VD indexes in the first two, and then focusing on their combination as proposed by Ribeiro Neto et al. (2021) in Section 4.1.3.

4.1.1 Standardized Precipitation Index (SPI)

According to Marengo et al. (2016), in the study period considered (1980-2018), a total of 9 droughts were registered in North-East Brazil: 1979-1981, 1982-1983, 1992-1993, 1997-1998, 2001-2002, 2005, 2007, 2010 and 2012-2015. This last drought has been then considered as connected with 2010's one, it continued with lower magnitude until 2018 (Marengo et al., 2018) and it is still not concluded . So, in the greater NEB area, approximately 52% out of 38 years included periods in drought conditions. The Banabuiú basin followed the same behavior, as seen in Figure 4.2, where the monthly SPI-12 results for the Banabuiú basin are shown. The shaded background areas represent the drought periods identified by Marengo et al. (2016). In each highlighted area (aside from 2007, which present an high variability across sub-basins) the index has values below 0, which means the occurrence of a dry period. Since the SPI index didn't consistently assume values above 0 after 2012, the region can be considered in a meteorological drought condition until 2018 (the end of this study's time window). 1992-1993 and the 2010-2018 are the most dry periods, with SPI values reaching and surpassing -2.

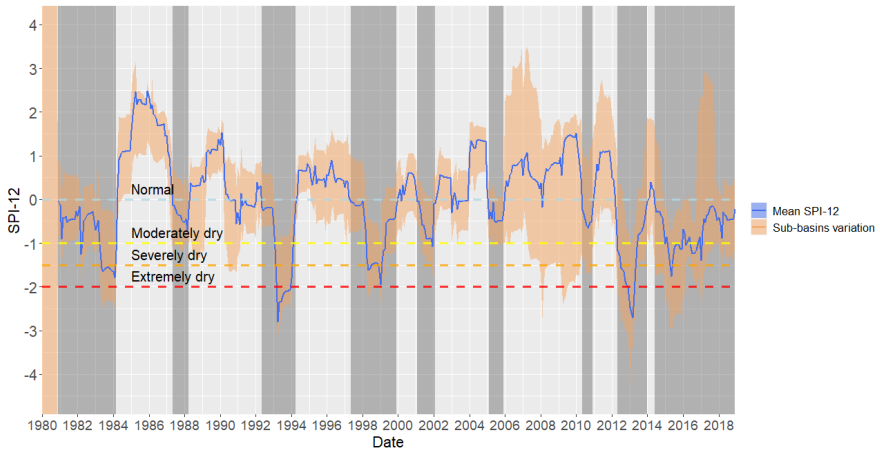

Figure 4.2: *Area of variation of SPI-12 computed on each sub-basin and mean over the whole basin. The shaded areas represent the drought periods as defined in Marengo et al. (2016), extending the 2010-2016 one until 2018. The dashed lines represent the SPI values boundaries for the meteorological conditions as defined in WMO (2012), Table 1.*

4.1.2 Volume Deviation (VD)

In Figure 4.3 the Volume Deviation computed for *AR* and *LR* scenarios is shown, highlighting the meteorological drought periods defined by negative SPI value. The VD series in Figure 4.3 (a) are related to Arrojado Lisboa's volume, as explained in Section 3.4.1, and are the ones used for the Drought Cycle Analysis, while Figure 4.3 (b) shows the mean of all the upstream reservoirs. Values below 0 indicate volume below half of the total capacity. It can be observed how the VD values decreases in correspondence to meteorological drought periods, after which the index tends towards positive values. Comparing the two scenarios in Figure 4.3 (a), it is clear that the presence of the DRN (dashed line in the graph) has an influence on Arrojado Lisboa's volume. It can be seen *before* the meteorological drought periods: the water stored before a drought is higher in the *LR* scenario. This reflects afterwards, in a slower transition towards a depletion condition of the reservoir (e.g. 1992, 1997). The influence can also be seen *during* and *between* drought events, as in 1996, 2013 and 2014, where the recharge is slower in presence of the DRN, leading the reservoir to be more susceptible to the next meteorological drought. In N and SR scenarios the other centralized reservoirs are removed (refer to Figure 4.1). This results in the overall higher volume in both scenarios (comparing Figure 4.3 (a) with Figure 4.3 (c)). Without the other big reservoirs, the effect of the network of small reservoirs on water storage is emphasized, with a higher mean difference between the two scenarios and an evident improved ability to recharge in the *Naturalized* scenario, as between 1996 and 2002.

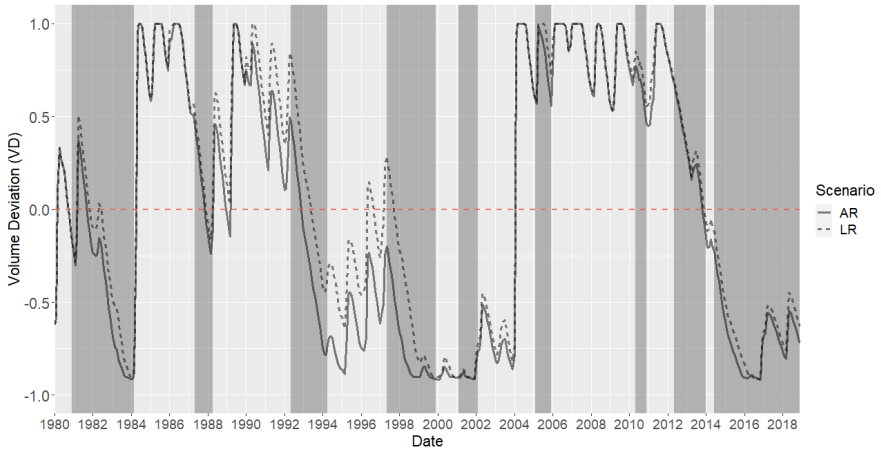

(a)

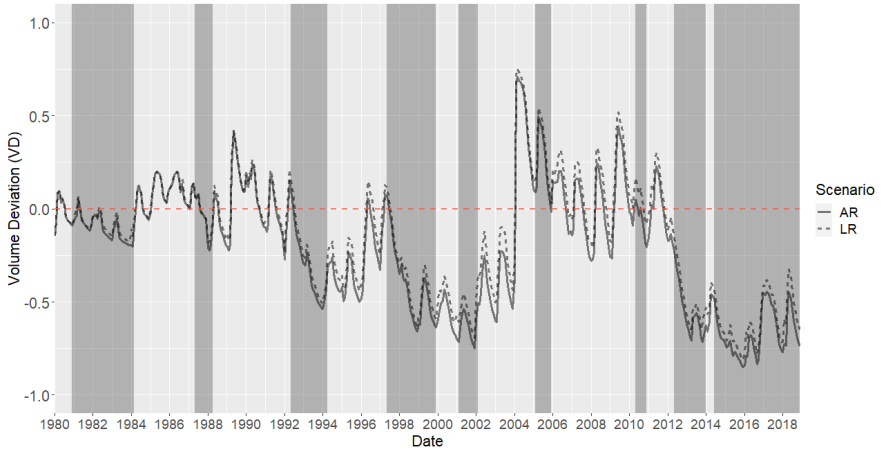

(b)

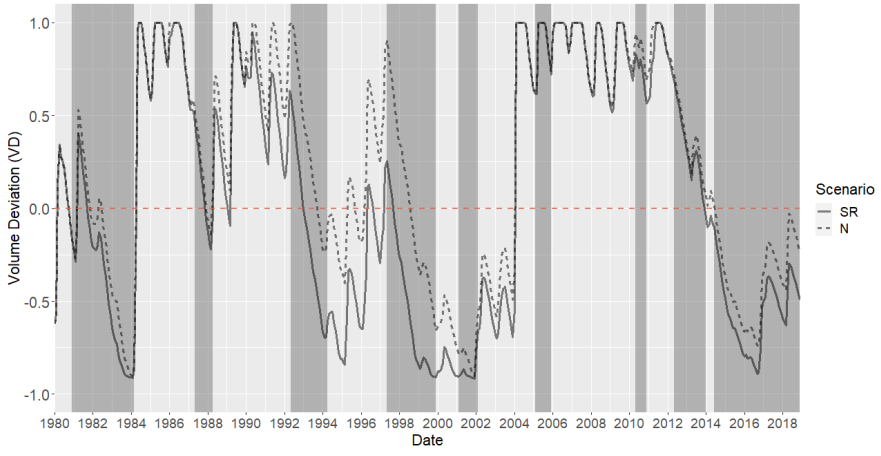

(c)

Figure 4.3: *Volume Deviation (VD) visualization. All Reservoirs and Large Reservoirs scenarios are shown in: (a) Arrojado Lisboa and (b) Average over all centralized reservoirs except Arrojado Lisboa. Naturalized and Small Reservoirs scenarios are shown in (c) Arrojado Lisboa*

The shaded areas indicate the meteorological drought periods in the Banabuiu catchment obtained extracting the months with SPI lower than 0 from the mean SPI shown in Figure 4.2.

4.1.3 Drought Cycle Analysis

In Table 4.1 are reported the percentages of months in the 4 drought phases explained in Section 3.4.1 in the four scenarios. It can be noted that both scenarios follow the same pattern across the 4 phases, but the *LR* scenario presents a lower percentage of months in drought conditions (71% against 75% of the *AR* scenario) compared to *AR*, which translates into 25 more months without hydrological-related droughts in *AR*, more than 2 years. A more in-depth observation can be made by comparing Phases 1 and 2 (non-occurence and meteorological drought), where the scenario with the small reservoirs (*AR*) has a lower percentage, and Phases 3 and 4, where it presents an higher percentage: the months missing from the meteorological drought state moved towards hydro-meteorological droughts (2% increase of Phase 3), while hydrological droughts extended over periods with non-occurrence of drought (4% increase of Phase 4). The absence of the large reservoirs enhances the increase in Phase 3 and 4 when the DRN is present: 5% and 6% respectively. The existence of the DRN thus extends the Phases 3 and 4 of droughts, with a higher increment in the pure hydrological drought, therefore stretching the duration of the drought events.

Table 4.1: *Percentage of months in the four drought phases in AR, LR, SR and N scenarios for Arrojado Lisboa*

	Percentage over total months			
Phase	AR [%]	LR [%]	SR [%]	N [%]
1. Non-occurence of drought	25	29	28	34
2. Meteorological drought	23	25	23	27
3. Hydro-meteorological drought	27	25	27	23
4. Hydrological drought	25	21	22	16
Total	100	100	100	100

In Figure 4.4, three main drought periods are represented showing the corresponding drought phases for each month in the two scenarios: 1992-1994, 1997-2002 and 2010-2018. On the horizontal bars are marked periods in which the influence of the DRN on drought evolution and intensity is particularly visible. In the first event, the *AR* scenario experiences an early shift towards the hydro-meteorological drought phase in May 1993, and the intensity remains higher until the end of the event. At the beginning of the second event (June 1997), the *AR* scenario is still in an hydrological drought condition, while the *LR* scenario recovered better from the previous drought event and was in a non-dry condition when the second event happened (Figure 4.3 (a) for reference). The drought intensity in this first year of the event is considerably higher in

the *AR* scenario, while afterwards they tend to become more similar. A similar behavior is seen also in the third event, where no changes of phases happen, but only an increase in intensity in the *AR* scenario. This visualization helps to confirm what has been observed previously: the existence of the DRN leads to faster transitions towards hydrological drought phases and also increases their intensity. The considerations made for the VD on the *N* and *SR* scenarios reflect on the complete DCA results shown in Figure 4.5. While in the first drought event the behavior of these scenarios is similar to the *AR* and *LR* ones (Figure 4.4), in the other two the influence of the DRN on drought evolution becomes clearer: *N* scenario slowly transitions towards the hydro-meteorological drought between 1997 and the end of 1998, while the *SR* is already in it from the start of 1998. In the last event the *N* scenario transitions faster towards the non-drought phase, both in 2014 and 2018.

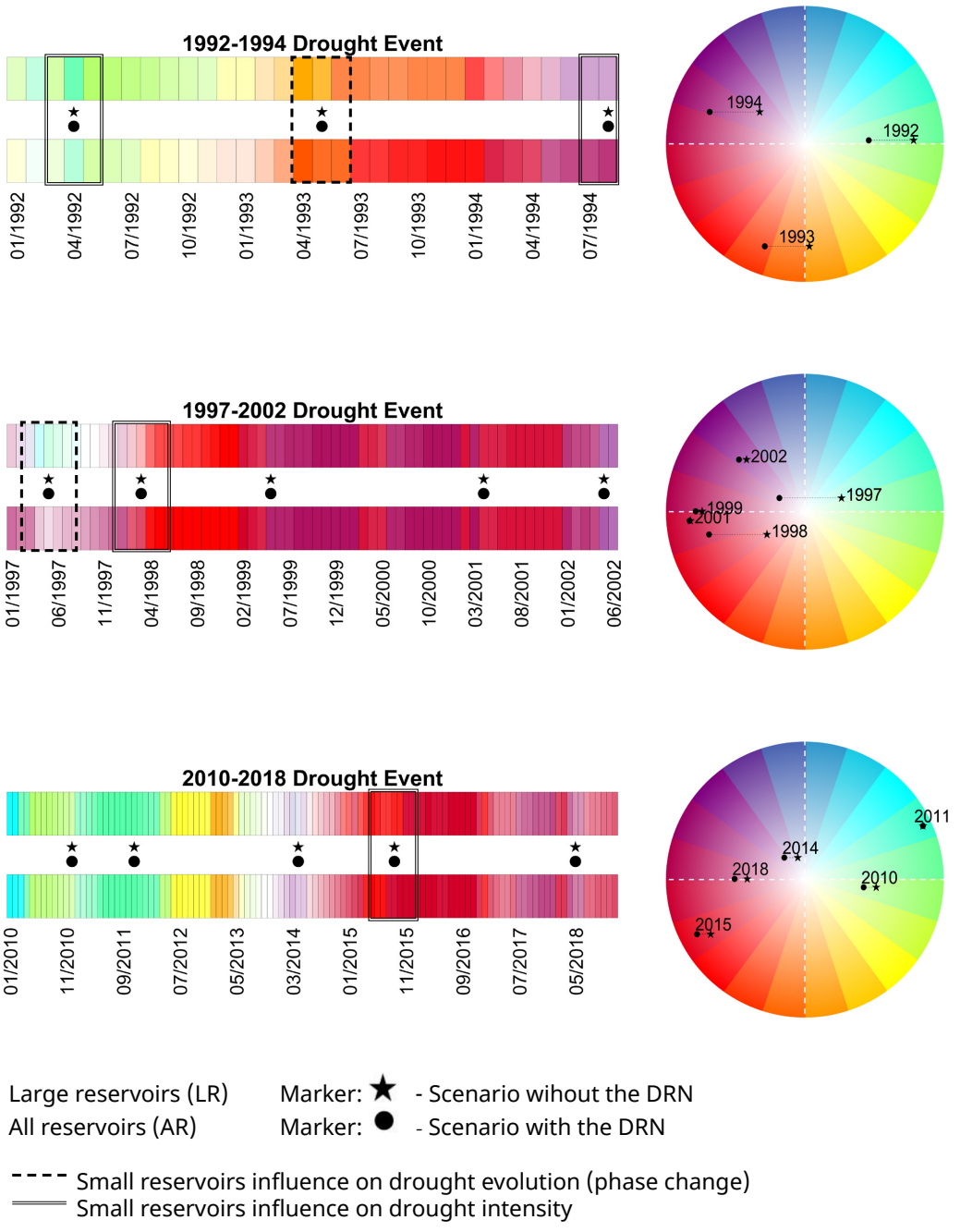

Figure 4.4: *Results of the Drought Cycle Analysis operated on Arrojado Lisboa in All Reservoirs and Large Reservoirs modeled scenarios for three main drought periods: 1992-1994, 1997-2002, 2010-2018. The colors of the horizontal bars align with the color of the Drought wheel, indicating the drought stage for each month. The markers between the horizontal bars are then plotted on the drought wheel. The distance between the two markers is the difference between the scenarios, showing the impact of the DRN.*

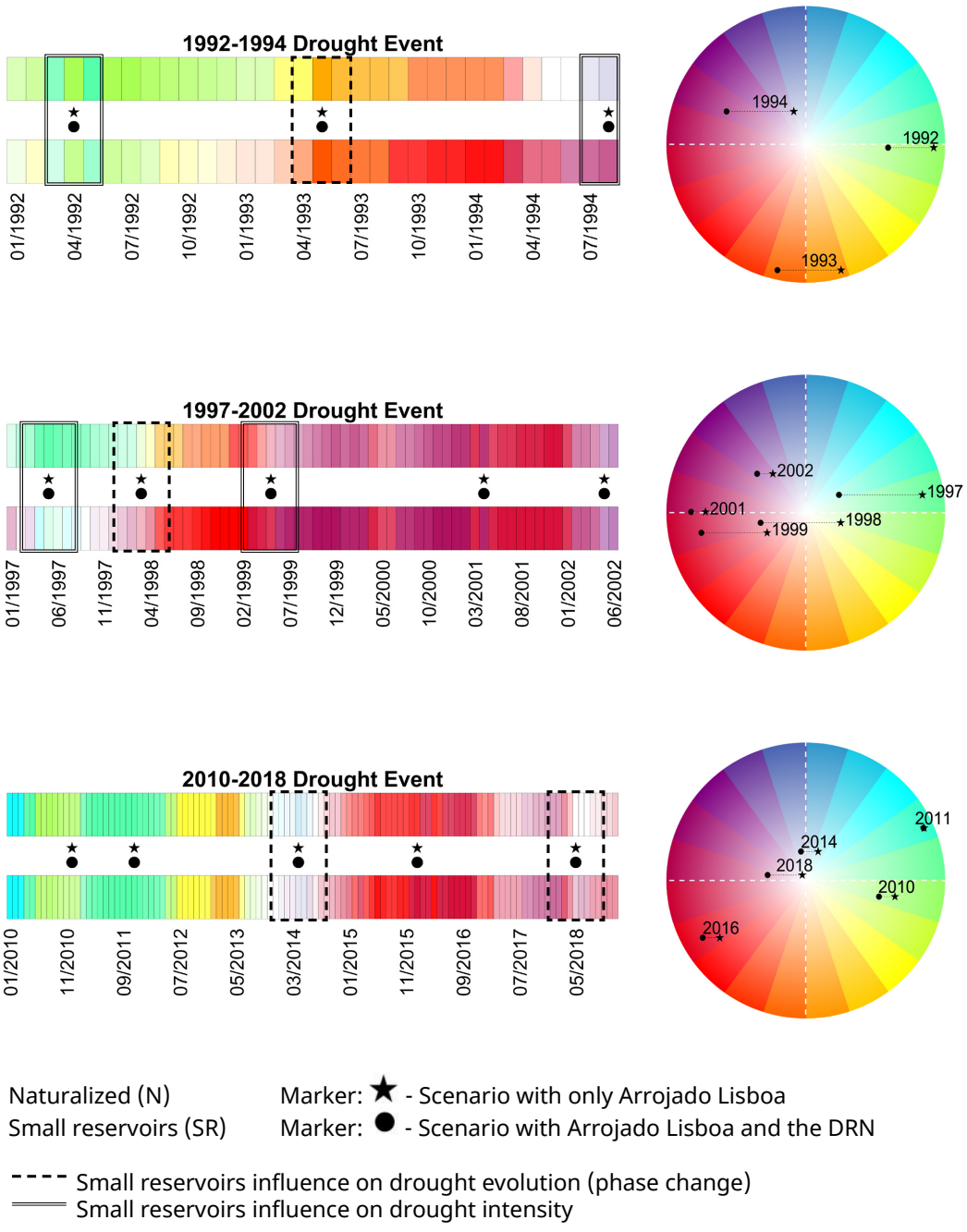

Figure 4.5: *Results of the Drought Cycle Analysis operated on Naturalized and Small Reservoirs scenarios for three main drought periods: 1992-1994, 1997-2002, 2010-2018. The colors of the horizontal bars align with the color of the Drought wheel, indicating the drought stage for each month. The markers between the horizontal bars are then plotted on the drought wheel. The distance between the two markers is the difference between the scenarios, showing the impact of the DRN.*

4.2 Downstreamness analysis outcomes

The results from the downstreamness analysis computed on the *AR* and *LR* scenarios are described in this Section starting from the D_{SC}, then moving to the D_{SV} and finally comparing them. The number of small reservoirs was assumed constant over time, as explained in Section 3.4.2.

4.2.1 Downstreamness of Storage Capacity

In Figure 4.6 the D_{SC} of the two scenarios are plotted. It has to be noted that the construction of the centralized reservoirs always decreased the D_{SC}, which may suggest an infrastructural planning towards a more diffused storage capacity in the basin. From the plot the effect of the existence of the DRN on the distribution of storage capacity in the basin (continuous line) can be clearly seen. The *AR* D_{SC}, compared to the scenario without small reservoirs, is decreased by an average of 3.7%, from a difference of 4.6% in 1980 to 3.2% in 2018, due to new construction of centralized reservoirs (the most important are indicated on the graph), which having an high relative weight decreases the relative weight of the smaller reservoirs in the downstreamness. The effect of the DRN therefore is to shift the distribution of the storage capacity to a relatively more upstream configuration than the one achievable with the centralized reservoirs alone.

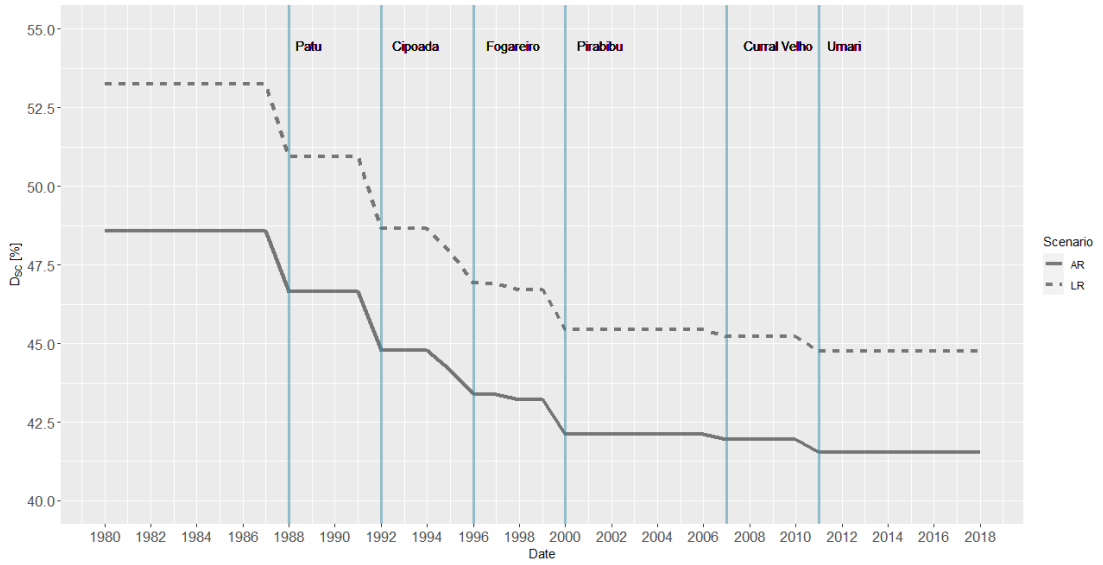

Figure 4.6: *Downstreamness of Storage Capacity (D_{SC}) comparison in All Reservoirs and Large Reservoirs modeled scenarios*

The lightblue lines indicate the construction of the reservoirs labeled next to the lines. The small reservoirs are assumed constant over time as explained in Section 3.4.2.

4.2.2 Downstreamness of Stored Volume

In Figure 4.7 the D_{SV} of the *AR* and *LR* scenarios are plotted. The *Large Reservoirs* scenario (dashed blue line) is relatively smoother than the *All Reservoirs* scenario: the presence of small reservoirs marginally increases the variability of the stored volume distribution in the basin (Coefficient of Variation equal to 13.51% in *LR* versus 13.66% in *AR*). This has a logical base, since without other reservoirs in place, the water will be only stored in the centralized reservoirs, which have less variability in their storage and management structure than small reservoirs. Without large reservoirs this effect is enhanced: the Coefficient of Variation difference between *SR* and *N* scenarios is 0.42%. The presence of the DRN can then increase stored volume variability across the basin, both before (2009) and during a drought event (2016), but the presence of a large reservoirs network can limit this effect.

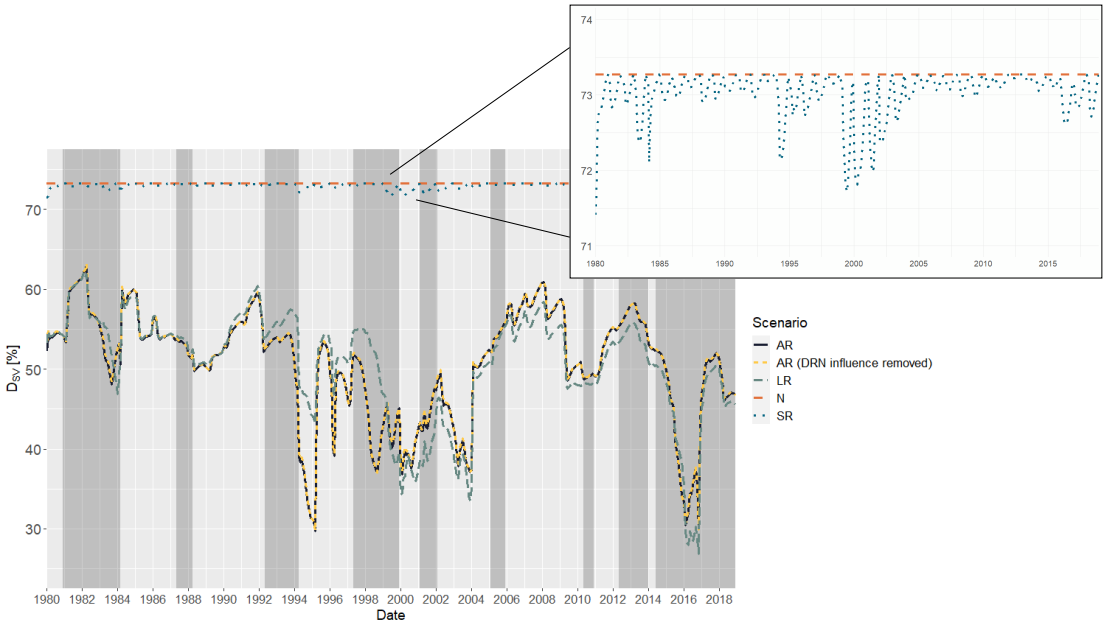

Figure 4.7: *Downstreamness of Stored Volume (D_{SV}) comparison in AR, LR, SR and N modeled scenarios. Zoom on SR and N scenarios' D_{SV} series*

The shaded areas indicate the meteorological drought periods in the Banabuiu catchment obtained extracting the months with SPI lower than 0 from the mean SPI shown in Figure 4.2.

Observing the difference between *N* and *SR* scenarios the direct influence of the DRN can be noted (Figure 4.7): the downstreamness of stored volume is lowered by the existence of the small reservoirs, with a maximum decrease of 1.55% in 1999, thus spreading the storage distribution through the basin. When large reservoirs are present, however, this direct effect is not clearly visible anymore: the *All Reservoirs* scenario retains a lower downstreamness until 2000,

but after 2000 its downstreamness surpasses the one of the *Large Reservoirs* scenario. In this period, the volume is thus more stored downstream in presence of the DRN, while in the period before, the opposite is observed. Rationally, if the water stored by small reservoirs is included (AR scenario), more storage would be located upstream, thus lowering the downstreamness of stored volume. To explain this counter-intuitive behavior of the results after 2000, the stored volume behavior has to be considered.

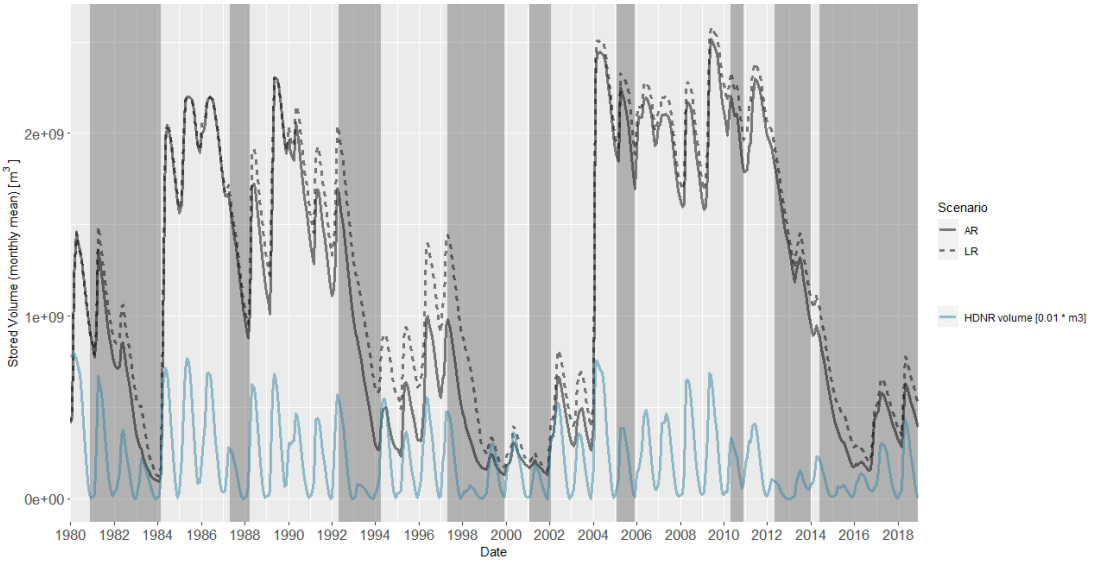

Figure 4.8: *Total stored volume comparison in All Reservoirs and Large Reservoirs modeled scenarios*

The shaded areas indicate the meteorological drought periods in the Banabuiu catchment obtained extracting the months with SPI lower than 0 from the mean SPI shown in Figure 4.2.

As shown in Figure 4.8, the overall stored volume in the basin is higher in the *LR* scenario. The DRN's contribution is 0.26% of the total stored volume in the *AR* scenario, with the centralized reservoirs covering the remaining 99.74%. The volume collected by the small reservoirs in the *AR* scenario is not able to even the volume collected by the centralized reservoirs while the DRN is missing. The *AR (DRN influence removed)* line in Figure 4.6 confirms that not considering the DRN in the calculation of the D_{SV} the result does not vary significantly from the complete calculation (RMSE of 0.18[1] between the two series.). It is then reasonable to assume that the reasons for the different and somewhat counter-intuitive results of the D_{SV} have to be searched in the behavior of the centralized reservoirs more than in the DRN. Around 1999 and 2000 the D_{SV} of the *LR* scenario became lower than *AR* scenario's one. From Figures 4.3 (a) it can be clearly seen that Arrojado Lisboa's volume is higher

[1]Computed on the D_{SV}, varying from 29.7 to 63.1%

in *LR* scenario, with a pronounced difference until approximately 1999, when the difference decreases (RMSE of 0.23 before 1999, 0.06 afterwards)[2]. Approximately in the same year, the difference between the average VD of the upstream reservoirs, Figure 4.3 (b), increases (RMSE varies from 0.04 to 0.08)[2]. Also, in the 5 years before 2000 4 centralized reservoirs were built, including Fogareiro, the third biggest reservoir in the basin (refer to Table 1.2), for an overall increase of 8.5 km^3 in the storage capacity (34% of the storage capacity before 1995): Arrojado Lisboa's relative high weight in D_x becomes more counterbalanced by stored volume upstream. Summarizing these considerations: around 2000 the upstream storage capacity grows; after '2000 Arrojado Lisboa's volume is approximately at the same level for both scenarios; at the same time the upstream centralized reservoirs have higher volumes in the *LR* scenario, which is not paired by the volume stored in the DRN in the *AR*. The result is a lower downstreamness of stored volume in the *Large Reservoirs* scenario after 2000.

D_{SC} and D_{SV} comparison In both scenarios, the D_{SV} is higher than the D_{SC} most of the time, as it can be seen in Figure 4.9. Referring to Figure 3.7, this indicates that, most of the time, in both scenarios the water is more stored downstream than upstream. The highest difference in the two scenarios can be seen in 1994, when the D_{SV} in the *AR* scenario reached a minimum of 30%, while in the *LR* scenario it remained around 45%.

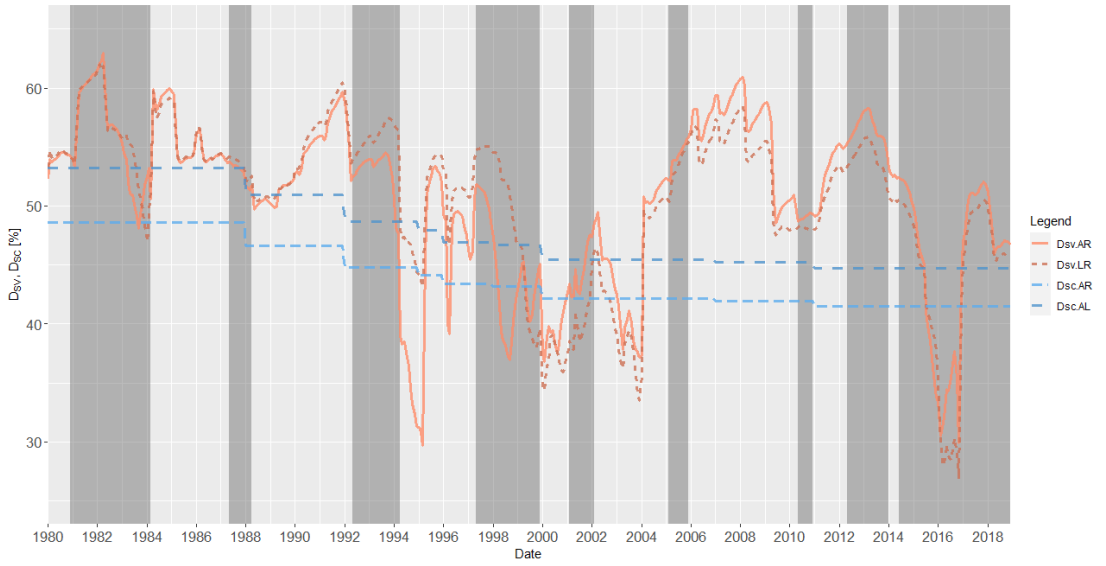

Figure 4.9: *Downstreamness of Stored Volume (D_{SV}) and Downstreamness of Storage Capacity (D_{SC}) comparison in All Reservoirs and Large Reservoirs modeled scenarios. The shaded areas indicate the meteorological drought periods in the Banabuiu catchment obtained extracting the months with SPI lower than 0 from the mean SPI shown in Figure 4.2.*

[2]Computed on the Volume Deviation for the considered reservoir, varying from -1 to 1 with no unit of measure.

4.3 Synthesis

Interesting aspects on the role of the DRN emerge from the results of the Drought Cycle Analysis and the Downstreamness analysis, plus observations on the stored volume. In time, the presence of the network of small reservoirs accelerates the transition towards hydrological drought phases and lengthens the recharge period in centralized reservoirs, thus increasing the length and intensity of the drought events (Figures 4.3 and 4.4). These influences have proven stronger when a network of big centralized reservoirs is missing (Figures 4.3 (c) and 4.5). In space, the DRN existence leads to a more upstream distribution of the storage capacity (Figure 4.6). When large reservoirs are missing, the DRN permits to store more volume upstream, reducing the D_{SV}. The low and highly variable actual stored volume retained in small reservoirs, however, results in a negligible direct influence on the downstreamness of stored volume when centralized reservoirs are instead present, leading to a higher dependency to their relative conditions (Figures 4.7 and 4.8).

5 Discussion

In this Chapter some points of discussion are described that have arisen during the study and others that could be implemented in future studies. The discussion is divided into topics regarding the results, the methodology followed and future possible studies.

5.1 Results discussion

Literature comparison It has been observed that storage of water in centralized reservoirs permits a delay in drought propagation from meteorological to hydrological drought (van Langen et al., 2021), which fits with the behavior of the scenario without the DRN observed in Section 4.1. In Ribeiro Neto et al. (2021) the Riacho do Sangue watershed (still in Ceará) is studied. Their results showed an influence of the DRN on the extension of hydrological related droughts, as well as an increase of the amount of water retained in the study area. In Section 4.2.2 it has been observed how the modeled scenario including the small reservoirs network has less overall stored volume, albeit having an higher overall storage capacity of the basin. As noted by Di Baldassarre et al. (2018), constructing can initially increase the supply of water, which in turn can increase the demand, creating a negative effect on water availability. Similar results to the performed downstreamness analysis for the Banabuiú basin are found in the ones computed by Colee (2018) and van Oel et al. (2018), which is here extended by computing it from 1980. The observed extension of the hydrological drought periods in Arrojado Lisboa (most downstream reservoir) in-

duced by the DRN finds a confirmation in van Oel et al. (2018), but to reach the same level of detail of the outcomes as that study and van Langen et al. (2021), where a correlation between downstream reservoirs and faster development of droughts is found, further analysis should be conducted.

Different effects depending on large reservoirs condition An interesting pattern has been found: depending on the storage condition in which the large reservoirs are at the beginning of the meteorological droughts, a different entity of the DRN effects is found. When the large reservoir is full or near the maximum capacity (VD $\geqslant$ 0.75) the difference between AR and LR scenarios is negligible, while with VD lower than 0.75 the difference becomes more visible. Two examples of both conditions are highlighted in Figure 5.1 regarding Arrojado Lisboa. This observation suggests that when the large reservoir is in a more depleted condition and a meteorological drought happens, the existence of a DRN will enhance the drought effects on the reservoir more than it would do if the reservoir would have been full. Having a better knowledge of this phenomenon may help the implementation of short term drought preparedness measures when the reservoirs are below a threshold (e.g. 75% of the maximum capacity).

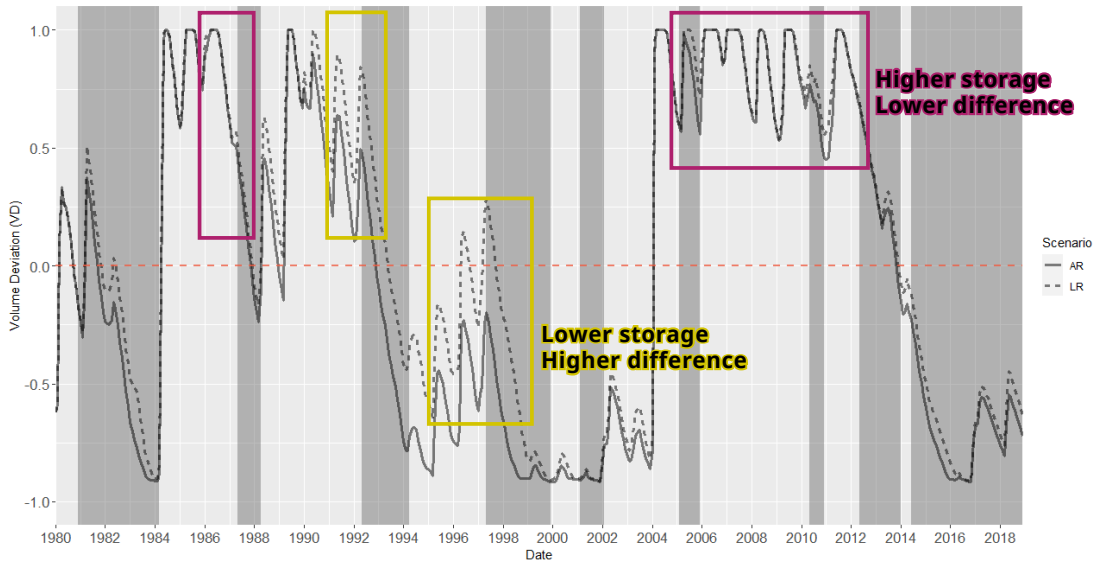

Figure 5.1: *Highlight on different magnitude of the DRN effect on Arrojado Lisboa's Volume Deviation*

Higher total stored volume without the DRN As observed in Figure 4.8, in the scenario without the DRN (*LR*) more overall volume is stored. This result is counter-intuitive, as more reservoirs would lead to more stored water. The volume

collected by the small reservoirs in the *All Reservoirs* scenario, however, is not able to even the volume collected by the centralized reservoirs while the DRN is missing. Aside from the water directly stored in the DRN there must be some significant losses and reductions in the potential yield of the large reservoirs. This gap can be explained by higher dispersion and transmission losses due to a more diffused network. The higher infiltration and evaporation rates in small reservoirs can also be a factor of the difference, as well as the retention of the catchment streamflow. The DRN has a highly variable nature and a limited storage capacity but its influence can go further than what it may seem: this phenomenon of lost potential yield has also to be investigated. For example, in Rabelo et al. (2021) a decrease in the catchment streamflow has been estimated, finding a greater impact in dry years.

5.2 Methodology discussion

Some aspects of the methodology followed are discussed here by separating into three main sections: data, model and analysis.

5.2.1 Data

Small reservoirs locations The data available for the geo-referencing of the small reservoirs composing the DRN is related to a survey performed by FUNCEME in 2020 (FUNCEME et al., 2021). Since no surveys were available for the previous years, this was the only information ready to be used, and it has been used to model the network as described in Section 3.2.3. The result is that temporal variation information of the number and even sizes of the small reservoirs is missing, and thus it is not considered in the model nor the analysis. The same number of reservoirs has been used throughout all the years: this strong approximation is still justified by the removal of approximately 7 thousands small reservoirs in the processing phase, equal to the 40% of all the reservoirs surveyed in 2020. In this study the temporal component of this data was not critical since the effects investigated were more general, considering the overall effects of the network's existence across 40 years. For studies focusing on shorter periods or on the effects generated by the DRN variation data with higher temporal resolution would be needed. Possible solutions to this issue could be performing new surveys on past satellite images (Nascimento and Ribeiro Neto, 2017), or estimating a coefficient of variation based on historical catalogs and then extrapolating the number of reservoirs for each year. This last hypothesis could be difficult due to the unregistered nature of most of the

small reservoirs, and since in dry years a higher rate of constructions can be expected (Krol et al., 2011; Di Baldassarre et al., 2018), the coefficient could vary over time.

5.2.2 Model

WASA-SED model's accounting of the DRN In the model's small reservoirs definition, smaller reservoirs are assumed to be located upstream of larger ones, which has been based on experience in dryland areas in Brazil and qualitative reasoning form topographic maps (Mamede et al., 2018; Güntner et al., 2004). This assumption is an approximation of the real condition, and the cascade routing operated through the classes may then not be always representative of the reality of the DRN. To avoid this approximation, though, the model should account for the position of all the single small reservoir, and then perform the water balance individually (in a similar way to what is done for the strategic reservoirs), which as stated in Section 3.3.1 is not feasible due to the uncontrolled and unmonitored nature of the small reservoirs, which makes the physical collection of their necessary parameters very difficult when the small reservoirs present are so numerous and diffused (Mamede et al., 2012). In smaller catchments with less dense networks this procedure could be applied, even though the possible gain in results obtainable or this increase in accuracy is not guaranteed to justify it. Rabelo et al. (2021) goes in this direction of representing in detail large and small reservoirs to analyse the cumulative impact of small reservoirs on the horizontal hydrological connectivity.

Possible model enhancements The mean performance of the WASA-SED model is satisfactory for the purpose of this thesis but it could be improved for analysis which need an higher detail quantitatively besides from the good dynamical representation which the model already provides. The possibilities of improvement are multiple: an higher temporal definition in the DRN characterization (Section 5.2.1), a renewed parameterization of the various components composing the block structure of the model (e.g. the Terrain Components) but also other aspects as the quantification of the water use (Bronstert et al., 2000; Güntner, 2002). Francke et al. (2018) proposes a method to quantify the effect of multiple model enhancements on the performance of the model.

Other possible models As Marahatta et al. (2021) underlines, in absence of direct measurements hydrological modeling is one of the best methods to estimate variable of interest as flow and volume. As pointed out in Addor and Melsen

(2019) the selection of a model should be based on its adequacy to the task (as it has been done in this thesis). WASA-SED as an hydrological model is feasible and ready to model a dense network of small reservoirs, as it already presents a module specifically for this task. Another promising and widely used large-scale model is MGB-IPH[1], made available from the Institute of Hydraulic Research of the Federal University of Rio Grande do Sul. Similarly to WASA-SED, the MGB model divides the hydrographic basin into small sub-basins, but its adaptability to the task of modeling an DRN hasn't been proved yet (Collischonn et al., 2007; De Paiva et al., 2013). The SWAT eco-hydrological model (Soil and Water Assessment Tool) is another candidate for the detailed representation and simulation of large and small reservoirs, in particular in catchments where water extraction and agriculture are relevant (Arnold et al., 2012; Rabelo et al., 2021).

5.2.3 Analysis

Downstreamness The downstreamness of stored volume (D_SV) results in AR and LR scenarios are not completely clear. An explanation to them has been provided by considering the stored volume variations in the two scenarios (Section 4.2.2), but other causes could be now unknown. The downstreamness could be computed and analysed also for each sub-catchment in the Banabuiú basin. This could provide higher resolution results on the whole basin, by describing in depth more local and diverse conditions. The different behaviors of the reservoirs throughout the basin in relation to the DRN can be analysed and observed to examine possible differences in the network's influence between upstream and downstream reservoirs. A pattern is also noted: when a meteorological drought happens, the D_{SV} tends towards lower values, thus moving the stored volume upstream. A further exploration of the causes behind this phenomenon may help describe better the influence of the DRN.

Further analyses involving N and SR scenarios The analyses here conducted can be further applied involving more the *Naturalized* and *Small Reservoirs* scenarios. The influence of the hydraulic structures and their operations on drought evolution can then be calculated excluding other influences. For example, from the VD in the N scenario the hydrological drought driven only by climate can be obtained. Afterwards the hydrological drought driven by small reservoirs can be obtained by the subtracting N from SR, the one driven by large reservoirs from $LR - N$, and the one driven by the combined effects of large and small

[1]MGB-IPH: Portuguese acronyms for Large Basin Model and Institute of Hydraulic Research

reservoirs from $AR - N$.

Other drivers consideration Water withdrawals time series from Arrojado Lisboa are not enough to fully explain the reservoir's observed volume variations (Figure 5.2). Other drivers could be involved in periods as 2006-2008, where withdrawals don't explain the volume decrease, which is not happening in the modeled simulations. Direct extractions from the reservoirs may be one of these drivers, for example extractions performed through water trucks or by mechanical pumps for households or commercial bottled water (de Lira Azevêdo et al., 2017). These sources of uncertainty in water management could be quantified or, if no data is available, estimated to obtain a more accurate view on the reservoirs variations and on human-induced droughts. In addition, periods of VD decrease happened and sometimes the VD remained negative without meteorological drought (Figure 4.3). Exploring additional drivers can help explaining how these patterns change and why.

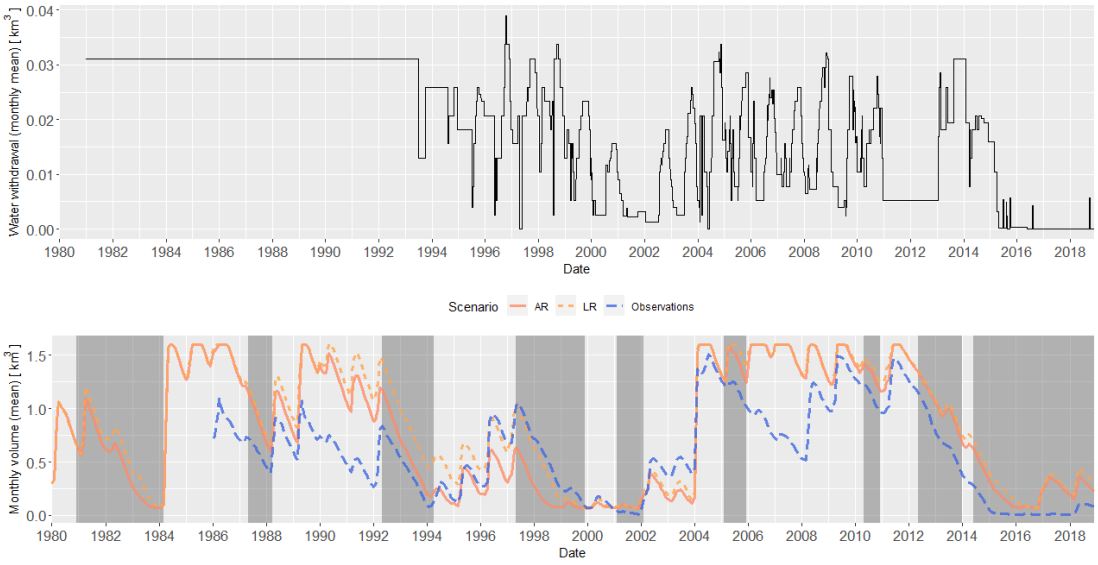

Figure 5.2: *Comparison between released volume and stored volume series for Arrojado Lisboa*

5.3 Future possible studies

Spatial Drought Cycle Analysis In order to explore the evolution through space of the drought phases, the Drought Cycle Analysis could be performed by including the spatial dimension together with the already considered time dimension. This can be performed by providing a representation of the basin with the information about the drought phases and intensities in the different areas of the

basin, e.g. in each sub-basin.

Cooperation scenario simulation To reduce the effects of the DRN on the centralized network of reservoirs, cooperation between the operators could be a viable path, for example following the Integrated Water Resource Management perspective (Network of Asian River Basin Organizations and UNESCO World Water Assessment Programme, 2009). Evidences in benefits from coordinated reservoir operations are highly documented, addressing optimization of economic, social and environmental issues (Castelletti et al., 2008), addressing for example flood mitigation (Seibert et al., 2014), or multi-objective and complex international scenarios (EU H2020, 2019). Different possibilities arise when dealing with existing infrastructure: operable reservoirs included in the DRN could be used as buffers to collect water from extreme events or used to distribute water in higher necessity periods, while the efficiency of some big centralized reservoirs could be questioned and rediscussed. Scenarios of cooperation could be already performed through the WASA-SED model. A set of alternatives to evaluate could include a change of status to the operable reservoirs included in the DRN, the definition of operational rules of the centralized reservoirs and the "new" operable reservoirs. The objectives of the scenario could be to minimize the hydrological drought phases length and to maximize the water distribution across the basin, in order to find a configuration which best fulfills these goals.

Policies considerations Alongside with simulations on the operational side of the mitigation of the DRN effects, a solution may arise from policies which improve meaningful public participation. Participatory management and plans involving local communities and other stakeholders can improve decision making at the river basin level, finding a balance between the need to decentralize water storage and the evidence that centralized reservoirs provide a more stable option in water storage (Lemos and de Oliveira, 2007; de Lira Azevêdo et al., 2017). A study on the policies and the existing realities in Ceará and in the Banabuiú basin could be useful to better understand how to address the existence and the impacts of the DRN on a less technical and more social level.

Climate change influence Climate change is unequivocal and will influence most environmental aspects both in the present, near and distant future (IPCC, 2021). Which role can the DRN play in this changing context? It has been observed that in the past its existence stretched the duration of hydrological drought periods in centralized reservoirs, and it is presumably that the same will happen

in the future if anything changes. On which degree this will happen is uncertain, due to various sources of uncertainty (Hattermann et al., 2018; Randall et al., 2007). Studies have already been done on projected climate change scenarios in semiarid areas (Zhao et al., 2014; Marengo et al., 2016), but exploring the impacts of the small reservoirs network in these future contexts can be useful to address the drought preparedness of the region and possible mitigation solutions (Gutiérrez et al., 2014).

6

Conclusions

Meteorological droughts have been registered in the semi-arid area of North-East Brazil since the sixteenth century. Between 1980 and 2018 approximately 52% of the years included a drought period, with the most sever ever drought occurring between 2010 and 2018 (Marengo et al., 2016, 2018). To adapt and prepare to the recurrent droughts small reservoirs have been built in the region (Rabelo et al., 2021), with 105,813 estimated reservoirs in the Ceará state alone (FUNCEME et al., 2021). The Banabuiú basin (19,530 km^2) follows the same pattern as its region with a mean density of 11.9 small reservoirs/km^2 which form a dense network of small reservoirs or Dense Reservoir Network (DRN), with areas reaching 40 small reservoirs/km^2 (Figure 3.2). Despite representing a small fraction on the total capacity in the area (7.1%), they have an important role in the water supply of small rural communities (Krol et al., 2011), as well as an influence in the hydrological drought evolution, which this study focused on.

To address the effect of the existence of a DRN on the drought evolution in the Banabuiú basin two scenarios have been simulated: one including all the small reservoirs and one with them removed. WASA-SED was the model selected for this task, a semi-distributed hydrological model able to simulate wide semi-arid areas considering both state-controlled centralized reservoirs and networks of diffused reservoirs (Güntner, 2002; Güntner et al., 2004; Mueller et al., 2010). To explore the DRN effects in time the Drought Cycle Analysis was performed, which makes it possible to compare the drought phase and in-

tensity in the two scenarios (Ribeiro Neto et al., 2021). To explore the effects in space, the Downstreamness Analysis was performed, assessing the changes in the distribution of the storage capacity and the stored volume throughout the basin (van Oel et al., 2018). The methodology followed has been proved successful to permit an assessment of the DRN influence on the hydrological drought evolution in a basin in time. Although having obtained some interesting information about the DRN's effect in the storage capacity spatial variation, the effects in space on the stored volume are instead not fully explained when large reservoirs are present. A more detailed analysis may then be needed to achieve this task, both in the representation of the small reservoirs network and in the dynamics between the network and the large reservoirs. In Rabelo et al. (2021), for example, this direction is taken.

Thanks to the Drought Cycle Analysis, the influence in time of the DRN in droughts' evolution was assessed as a 2% increase in hydro-meteorological drought periods and a 4% increase in hydrological drought periods. This effect is linked to observed patterns in the Volume Deviation difference between scenarios: the presence of the DRN leads to slower recharge of the large centralized reservoirs between and during drought events, which results in a faster transition towards hydrological drought phases. Another pattern has been discussed, which links lower volume level in large reservoirs to higher impacts from the DRN when a meteorological drought starts. These influences are enhanced when the large reservoirs are removed from the basin. The presence of a large reservoirs network acts then as an attenuator of the DRN effects in time. The Downstreamness Analysis permitted to assess an increase in the upstream distribution of the storage capacity in the basin by an average of 3.7% when the DRN is present. The influence of the small reservoirs network on stored volume distribution in the basin is an increase in the upstream stored volume when large reservoirs are removed: when they are present, the DRN effect is instead not directly explainable from the analysis conducted, and the distribution of the stored volume across the basin is more dependent on large reservoirs relative conditions. Another influence of the DRN is found in a relatively higher variability in the volume distribution. These considerations have been discussed, and a more detailed analysis on the causes of the stored volume and D_{SV} behaviors is needed to fully understand them.

The role of the DRN on the evolution of droughts is multifaceted: in time it increases the incidence and the intensity of hydrological drought phases, in space it increases the upstream storage capacity but it may lead upstream large

reservoirs to store less water, leading them to potentially higher drought impacts. It is then useful to further explore the relationships between the effects in time and space, deepening the knowledge about the influences of the DRN and the causes behind the effects here identified through future studies and analyses. The results may help the implementation of drought preparedness and adaptation measures in the Banabuiú basin and in other similar conditions both in North-East Brazil and other semi-arid areas.

Bibliography

N. Addor and L. A. Melsen. Legacy, Rather Than Adequacy, Drives the Selection of Hydrological Models. *Water Resources Research*, 55(1):378–390, jan 2019. ISSN 1944-7973. doi: 10.1029/2018WR022958.

J. G. Arnold, D. N. Moriasi, P. W. Gassman, K. C. Abbaspour, M. J. White, R. Srinivasan, C. Santhi, R. D. Harmel, A. van Griensven, M. W. V. Liew, N. Kannan, and M. K. Jha. SWAT: Model Use, Calibration, and Validation. *Transactions of the ASABE*, 55(4):1491–1508, jul 2012. ISSN 21510032. doi: 10.13031/2013.42256.

S. Beguería and S. M. Vicente-Serrano. Package 'SPEI'. Technical report, CRAN Repository, 2017. URL `http://sac.csic.es/spei`.

R. Bivand, T. Keitt, and B. Rowlingson. Package 'rgdal' -Bindings for the 'Geospatial' Data Abstraction Library. Technical report, CRAN Repository, 2021. URL `http://rgdal.r-forge.r-project.org/`.

A. Bronstert, A. Jaeger, A. Güntner, M. Hauschild, P. Döll, and M. Krol. Integrated modelling of water availability and water use in the semi-arid Northeast of Brazil. *Physics and Chemistry of the Earth, Part B: Hydrology, Oceans and Atmosphere*, 25(3):227–232, 2000. doi: 10.1016/S1464-1909(00)00008-3.

A. Castelletti, F. Pianosi, and R. Soncini-Sessa. Water reservoir control under economic, social and environmental constraints. *Automatica*, 44(6):1595–1607, 2008. ISSN 00051098. doi: 10.1016/j.automatica.2008.03.003.

CIAT. CGIAR-CSI SRTM - SRTM 90m DEM Digital Elevation Database, 2021. URL `https://srtm.csi.cgiar.org/`.

COGERH, SOHIDRA, and FUNCEME. Atlas dos Recursos Hídricos do Ceará. URL `http://atlas.cogerh.com.br/`.

M. Colee. The Downstreamness of Consumptive Water Use, 2018.

W. Collischonn, D. Allasia, B. C. da Silva, and C. E. Tucci. The MGB-IPH model for large-scale rainfall-runoff modelling. *Hydrological Sciences Journal*, 52(5):878–895, 2007. ISSN 02626667. doi: 10.1623/hysj.52.5.878.

E. de Lira Azevêdo, R. R. N. Alves, T. L. P. Dias, and J. Molozzi. How do people gain access to water resources in the Brazilian semiarid (Caatinga) in times of climate change? *Environmental Monitoring and Assessment*, 189(8), aug 2017. doi: 10.1007/S10661-017-6087-Z.

R. C. D. De Paiva, D. C. Buarque, W. Collischonn, M. P. Bonnet, F. Frappart, S. Calmant, and C. A. Bulhões Mendes. Large-scale hydrologic and hydrodynamic modeling of the Amazon River basin. *Water Resources Research*, 49(3):1226–1243, 2013. ISSN 19447973. doi: 10.1002/wrcr.20067.

G. Di Baldassarre, N. Wanders, A. AghaKouchak, L. Kuil, S. Rangecroft, T. I. Veldkamp, M. Garcia, P. R. van Oel, K. Breinl, and A. F. Van Loon. Water shortages worsened by reservoir effects. *Nature Sustainability*, 1(11):617–622, 2018. ISSN 23989629. doi: 10.1038/s41893-018-0159-0.

EU H2020. DAFNE - A Decision-Analytic Framework to explore the water-energy-food NExus in complex transboundary water resources systems of fast growing developing countries. Technical Report Deliverable D5.1, 2019.

T. Francke, G. Baroni, A. Brosinsky, S. Foerster, J. A. López-Tarazón, E. Sommerer, and A. Bronstert. What Did Really Improve Our Mesoscale Hydrological Model? A Multidimensional Analysis Based on Real Observations. *Water Resources Research*, 54(11):8594–8612, nov 2018. ISSN 19447973. doi: 10.1029/2018WR022813.

FUNCEME. Portal Hidrológico do Ceará. URL http://www.hidro.ce.gov.br/.

FUNCEME, M. R. de Freitas Filho, and M. S. Benicio de Souza Carvalho. Mapeamento das barragens dos pequenos reservatórios d'água situados no Estado do Ceará. Technical report, Governo do Estado do Ceará, 2021.

W. H. Green and G. A. Ampt. Studies on Soil Phyics. *The Journal of Agricultural Science*, 4(1):1–24, 1911. ISSN 1469-5146. doi: 10.1017/S0021859600001441. URL https://www.cambridge.org/core/journals/journal-of-agricultural-science/article/abs/studies-on-soil-phyics/6EE03D61E70FCEFD6EAE4D59BFCC1FF9.

A. Güntner. *Large-scale hydrological modelling in the semi-arid North-East of Brazil*. PhD thesis, Potsdam Institute for Climate Impact Research, 2002. URL https://publishup.uni-potsdam.de/opus4-ubp/frontdoor/deliver/index/docId/59/file/guentner.pdf.

A. Güntner, M. S. Krol, J. C. D. Araújo, and A. Bronstert. Simple water balance modelling of surface reservoir systems in a large data-scarce semiarid region. *Hydrological Sciences Journal*, 49(5), 2004. ISSN 0262-6667. doi: 10.1623/hysj.49.5.901.55139.

A. Güntner, E. N. Müller, G. Mamede, T. Francke, P. Medeiros, T. Pilz, and E. Rottler. WASA-SED | User manual, 2021. URL https://tillf.github.io/WASA-SED/.

A. P. A. Gutiérrez, N. L. Engle, E. De Nys, C. Molejón, and E. S. Martins. Drought preparedness in Brazil. *Weather and Climate Extremes*, 3:95–106, 2014. ISSN 22120947. doi: 10.1016/j.wace.2013.12.001.

F. F. Hattermann, T. Vetter, L. Breuer, B. Su, P. Daggupati, C. Donnelly, B. Fekete, F. Florke, S. N. Gosling, P. Hoffmann, S. Liersch, Y. Masaki, Y. Motovilov, C. Muller, L. Samaniego, T. Stacke, Y. Wada, T. Yang, and V. Krysnaova. Sources of uncertainty in hydrological climate impact assessment: A cross-scale study. *Environmental Research Letters*, 13(1), 2018. ISSN 17489326. doi: 10.1088/1748-9326/aa9938.

M. Hayes, M. Svoboda, N. Wall, and M. Widhalm. The Lincoln Declaration on drought indices: Universal meteorological drought index recommended. *Bulletin of the American Meteorological Society*, 92(4):485–488, 2011. ISSN 00030007. doi: 10.1175/2010BAMS3103.1.

R. J. Hijmans. Package 'raster' - Geographic Data Analysis and Modeling. Technical report, CRAN Repository, 2021. URL https://github.com/rspatial/raster/.

IBGE. Atlas do Censo Demográfico 2010, 2010. URL https://censo2010.ibge.gov.br/apps/atlas/.

IBGE. Regional Divisions of Brazil, 2017. URL https://www.ibge.gov.br/en/geosciences/territorial-organization/regional-division/21536-regional-divisions-of-brazil.html.

IPCC. Summary for Policymakers. Technical report, 2021. URL https://www.ipcc.ch/report/ar6/wg1/.

V. Klemeš. Operational testing of hydrological simulation models. *Hydrological Sciences Journal*, 31(1): 13–24, 1986. ISSN 2150-3435. doi: 10.1080/02626668609491024.

W. J. Knoben, J. E. Freer, and R. A. Woods. Technical note: Inherent benchmark or not? Comparing Nash-Sutcliffe and Kling-Gupta efficiency scores. *Hydrology and Earth System Sciences*, 23(10):4323–4331, oct 2019. doi: 10.5194/HESS-23-4323-2019.

M. S. Krol, M. J. de Vries, P. R. van Oel, and J. C. de Araújo. Sustainability of Small Reservoirs and Large Scale Water Availability Under Current Conditions and Climate Change. *Water Resources Management*, 25(12):3017–3026, 2011. ISSN 09204741. doi: 10.1007/s11269-011-9787-0.

M. C. Lemos and J. L. F. de Oliveira. Water Reform across the State/Society Divide: The Case of Ceará, Brazil. *Water Resources Development*, 21(1):133–147, mar 2007. doi: 10.1080/0790062042000316857.

G. L. Mamede. *Sedimentation Modelling and Sediment Management in Reservoirs of Dryland Catchments*. PhD thesis, University of Potsdam, Potsdam, 2008. URL https://publishup.uni-potsdam.de/opus4-ubp/frontdoor/deliver/index/docId/1546/file/mamede_diss.pdf.

G. L. Mamede, N. A. M. Araújo, C. M. Schneider, J. C. de Araújo, and H. J. Herrmann. Overspill avalanching in a dense reservoir network. *Proceedings of the National Academy of Sciences*, 109(19):7191–7195, may 2012. ISSN 0027-8424. doi: 10.1073/PNAS.1200398109.

G. L. Mamede, A. Guentner, P. H. A. Medeiros, J. C. de Araújo, and A. Bronstert. Modeling the Effect of Multiple Reservoirs on Water and Sediment Dynamics in a Semiarid Catchment in Brazil. *Journal of Hydrologic Engineering*, 23(12):05018020, 2018. ISSN 1084-0699. doi: 10.1061/(asce)he.1943-5584.0001701.

S. Marahatta, L. Devkota, and D. Aryal. Hydrological Modeling: A Better Alternative to Empirical Methods for Monthly Flow Estimation in Ungauged Basins. *Journal of Water Resource and Protection*, 13(3): 254–270, mar 2021. doi: 10.4236/JWARP.2021.133015.

J. A. Marengo, R. R. Torres, and L. M. Alves. Drought in Northeast Brazil - past, present, and future. *Theoretical and Applied Climatology*, 129(3-4):1189–1200, 2016. ISSN 14344483. doi: 10.1007/s00704-016-1840-8. URL http://dx.doi.org/10.1007/s00704-016-1840-8.

J. A. Marengo, L. M. Alves, R. C. Alvala, A. P. Cunha, S. Brito, and O. L. Moraes. Climatic characteristics of the 2010-2016 drought in the semiarid northeast Brazil region. *Anais da Academia Brasileira de Ciencias*, 90(2):1973–1985, 2018. ISSN 16782690. doi: 10.1590/0001-3765201720170206.

S. Mirzaei, M. Raoof, A. Ghasemi, H. Etaati, M. Moradnezhadi, and Y. Mirzaei. Determination of A Some Simple Methods for Outlier Detection in Maximum Daily Rainfall (Case Study: Baliglichay Watershed Basin – Ardebil Province – Iran). *BEPLS Bull. Env. Pharmacol. Life Sci*, 3(33):110–117, 2014. URL http://www.bepls.com/feb_2014/17.pdf.

F. Molle. *Geometria dos Pequenos Acudes*, volume 53. 1994. ISBN 9788578110796.

S. Moritz. *Package 'imputeTS'. Time Series Missing Value Imputation*. Number 3.2. 2021. ISBN 9789751135247. doi: 10.32614/RJ-2017-009. URL https://journal.r-project.org/archive/2017/RJ-2017-009/index.html.

E. N. Mueller, A. Güntner, T. Francke, and G. Mamede. Modelling sediment export, retention and reservoir sedimentation in drylands with the WASA-SED model. *Geoscientific Model Development*, 3(1):275–291, 2010. doi: 10.5194/GMD-3-275-2010.

V. F. Nascimento and A. Ribeiro Neto. Characterization of reservoirs for water supply in Northeast Brazil using high resolution remote sensing. *Rbrh*, 22(0), 2017. ISSN 2318-0331. doi: 10.1590/2318-0331.0217170060.

Network of Asian River Basin Organizations and UNESCO World Water Assessment Programme. *IWRM guidelines at river basin level, part 1: principles*. UNESCO, 2009. ISBN 978-92-3-104100-6.

L. R. Oldeman and V. W. van Engelen. A world soils and terrain digital database (SOTER) — An improved assessment of land resources. *Geoderma*, 60(1-4):309–325, dec 1993. ISSN 0016-7061. doi: 10.1016/0016-7061(93)90033-H.

J.-F. Pekel, A. Cottam, N. Gorelick, and A. S. Belward. High-resolution mapping of global surface water and its long-term changes. *Nature*, 540(7633):418–422, dec 2016. ISSN 1476-4687. doi: 10.1038/nature20584.

U. P. Rabelo, J. Dietrich, A. C. Costa, M. N. Simshäuser, F. E. Scholz, V. T. Nguyen, and I. E. Lima Neto. Representing a dense network of ponds and reservoirs in a semi-distributed dryland catchment model. *Journal of Hydrology*, 603:127103, dec 2021. ISSN 0022-1694. doi: 10.1016/J.JHYDROL.2021.127103.

R. P. L. Ramos. Precipitation characteristics in the Northeast Brazil dry region. *Journal of Geophysical Research*, 80(12):1665–1678, apr 1975. ISSN 2156-2202. doi: 10.1029/jc080i012p01665.

D. Randall, R. Wood, S. Bony, R. Colman, T. Fichefet, J. Fyfe, V. Kattsov, A. Pitman, J. Shukla, J. Srinivasan, R. Stouffer, A. Sumi, and K. Taylo. Climate Models and Their Evaluation. *Climate Change 2007: The Physical Science Basis. Contribution of Working Group I to the Fourth Assessment Report of the Intergovernmental Panel on Climate Change*, 323:589–662, 2007. ISSN 09609822. doi: 10.1016/j.cub.2007.06.045.

G. G. Ribeiro Neto, L. A. Melsen, E. S. P. R. Martins, and D. W. Walker. Drought Cycle Analysis to evaluate the influence of small reservoirs on drought evolution, 2021.

D. T. Rodrigues, W. A. Gonçalves, M. H. C. Spyrides, . Cláudio, M. Santos E Silva, and D. O. De Souza. Spatial distribution of the level of return of extreme precipitation events in Northeast Brazil. *International Journal of Climatology*, 2020. doi: 10.1002/joc.6507.

P. J. Rousseeuw and M. Hubert. Robust statistics for outlier detection. *Wiley Interdisciplinary Reviews: Data Mining and Knowledge Discovery*, 1(1):73–79, jan 2011. ISSN 1942-4795. doi: 10.1002/WIDM.2.

P. J. Rousseeuw and M. Hubert. Anomaly detection by robust statistics. *Wiley Interdisciplinary Reviews: Data Mining and Knowledge Discovery*, 8(2), mar 2018. doi: 10.1002/WIDM.1236.

S. P. Seibert, D. Skublics, and U. Ehret. The potential of coordinated reservoir operation for flood mitigation in large basins-A case study on the Bavarian Danube using coupled hydrological-hydrodynamic models. 2014. doi: 10.1016/j.jhydrol.2014.06.048.

Z. Sen. Average Areal Precipitation by Percentage Weighted Polygon Method. *Journal of Hydrologic Engineering*, 3(1):69–72, 1998. doi: 10.1061/(ASCE)1084-0699(1998)3:1(69).

W. J. Shuttleworth and J. S. Wallace. Evaporation from sparse crops-an energy combination theory. *Quarterly Journal of the Royal Meteorological Society*, 111(469):839–855, jul 1985. ISSN 1477-870X. doi: 10.1002/QJ.49711146910.

A. B. Souza, H. B. M Oliveira, R. S. França, A. C. Costa, R. F. V Silva, and E. S. P R Martins. Geração automatizada de dados de entrada para o modelo WASA-SED. In *XX Simpósio Brasileiro de Recursos Hídricos*, 2013.

R. Turner. Package 'deldir' - Delaunay Triangulation and Dirichlet (Voronoi) Tessellation. Technical report, CRAN Repository, 2021.

B. Uniyal, J. Dietrich, N. Q. Vu, M. K. Jha, and J. L. Arumí. Simulation of regional irrigation requirement with SWAT in different agro-climatic zones driven by observed climate and two reanalysis datasets. *Science of the Total Environment*, 649:846–865, 2019. ISSN 18791026. doi: 10.1016/j.scitotenv.2018.08.248.

S. C. van Langen, A. C. Costa, G. G. Ribeiro Neto, and P. R. van Oel. Effect of a reservoir network on drought propagation in a semi-arid catchment in Brazil. *Hydrological Sciences Journal*, 2021. doi: 10.1080/02626667.2021.1955891.

P. van Oel. *Water-scarcity patterns : spatiotemporal interdependencies between water use and water availability in a semi-arid river basin*. PhD thesis, University of Twente, Enschede, The Netherlands, 2009. URL `https://research.utwente.nl/en/publications/water-scarcity-patterns-spatiotemporal-interdependencies-between--2`.

P. R. van Oel, M. S. Krol, and A. Y. Hoekstra. Downstreamness: A Concept to Analyze Basin Closure. *Journal of Water Resources Planning and Management*, 137(5):404–411, 2011. ISSN 0733-9496. doi: 10.1061/(asce)wr.1943-5452.0000127.

P. R. van Oel, E. S. Martins, A. C. Costa, N. Wanders, and H. A. van Lanen. Diagnosing drought using the downstreamness concept: the effect of reservoir networks on drought evolution. *Hydrological Sciences Journal*, 63(7):979–990, 2018. ISSN 21503435. doi: 10.1080/02626667.2018.1470632.

WMO. Standardized Precipitation Index User Guide. Technical report, World Meteorological Organization (WMO), Geneva, Switzerland, 2012. URL `https://public.wmo.int/en/resources/library/standardized-precipitation-index-user-guide`.

E. Wu, W. Liu, and S. Chawla. Spatio-temporal outlier detection in precipitation data. *Lecture Notes in Computer Science (including subseries Lecture Notes in Artificial Intelligence and Lecture Notes in Bioinformatics)*, 5840 LNCS:115–133, 2010. ISSN 03029743. doi: 10.1007/978-3-642-12519-5_7.

M. Zaniolo, M. Giuliani, A. F. Castelletti, and M. Pulido-Velazquez. Automatic design of basin-specific drought indexes for highly regulated water systems. *Hydrology and Earth System Sciences*, 22(4):2409–2424, 2018. ISSN 16077938. doi: 10.5194/hess-22-2409-2018.

C. Zhao and J. Yang. A Robust Skewed Boxplot for Detecting Outliers in Rainfall Observations in Real-Time Flood Forecasting. *Advances in Meteorology*, 2019:1–8, 2019. ISSN 16879317. doi: 10.1155/2019/1795673.

T. Zhao, L. Chen, and Z. Ma. Simulation of historical and projected climate change in arid and semiarid areas by CMIP5 models. *Chinese Science Bulletin*, 59(4):412–429, 2014. ISSN 10016538. doi: 10.1007/s11434-013-0003-x.

A

List of Acronyms

ANA: Agência Nacional de Águas e Saneamento Básico
AR: All Reservoirs scenario
CDD: Consecutive Dry Days
CGIAR: Consultative Group for International Agricultural Research
DEM: Digital Elevation Model
DCA: Drought Cycle Analysis
DRN: Dense Reservoir Network
D_{SC}: Downstreamness of Storage Capacity
D_{SV}: Downstreamness of Stored Volume
FUNCEME: Fundação Cearense de Meteorologia e Recursos Hídricos
INMET: Instituto National de Meteorologia
LR: Large Reservoirs scenario
N: Naturalized scenario
NEB: North-East Brazil
PI: Precipitation Index
SESAM: Sediment Export from Semi-Arid Catchments: Measurement and Modelling
SPI: Standardized Precipitation Index
SR: Small Reservoirs scenario
VD: Volume Deviation
WASA-SED: Water Availability in Semi-Arid environments-SEDiments
WMO: World Meteorological Organization
WSI: Water Scarcity Index

B

Additional tables

Table B.1: *WASA-SED scaling factors resulting from the calibration*

Calibrated scaling factors					
Sub-basin ID	**Value**	**Sub-basin ID**	**Value**	**Sub-basin ID**	**Value**
123	3.6	143	5.6	152	2.4
125	6.8	144	1	153	0.6
126	1.4	145	1.8	154	2.4
127	0.4	146	0.2	155	1
134	1	147	0.8	156	0.8
137	1	148	1.2	157	0.8
138	4.2	149	2	158	3
139	1	150	1.6	159	2
142	1.6	151	0.6	160	0.2

Table B.2: *DRN classification as input to the WASA-SED model*

	Reservoir class				
Sub-basin ID	**1**	**2**	**3**	**4**	**5**
123	511	165	56	52	97
125	119	34	21	13	19
126	133	52	21	8	15
127	104	28	10	3	6
134	238	78	24	26	36
137	332	90	35	28	27
138	20	9	2	2	4
139	234	72	23	17	25
142	165	69	15	14	20
143	522	148	43	34	58
144	390	83	28	13	24
145	179	20	8	3	6
146	16	2	0	1	1
147	102	21	7	13	14
148	52	10	6	1	3
149	578	125	19	27	24
150	332	96	20	21	15
151	88	22	4	7	2
152	13	6	1	1	2
153	68	7	0	0	0
154	18	1	3	2	0
155	922	195	47	44	44
156	725	180	64	43	72
157	317	95	31	25	24
158	237	37	20	15	27
159	371	80	23	19	14
160	182	61	14	15	19

Table B.3: *WASA-SED model performances for each sub-basin, with run performed on the whole period 1980 - 2018*

Sub-basin ID	R^2	NSE	PBIAS	KGE	NRMSE
123	0.95	0.93	-5	0.9	0.07
125	0.71	0.64	-19.7	0.73	0.19
126	0.74	0.7	-7.1	0.83	0.12
127	0.91	0.89	0.1	0.8	0.09
138	0.24	-15.18	-99.5	-1.03	0.67
142	0.42	0.12	9.1	0.59	0.31
143	0.16	-0.81	-23.9	0.32	0.41
145	0.44	0.31	-10.7	0.64	0.23
146	0.17	-0.38	53.6	0.2	0.38
147	0.64	0.51	-2	0.74	0.18
148	0.35	0.23	-8	0.57	0.32
149	0.32	0.03	5.4	0.55	0.3
150	0.5	0.4	-7.7	0.7	0.26
151	0.63	0.46	-8	0.71	0.23
152	0.69	0.68	7.2	0.79	0.17
153	0.27	-0.27	-10.6	0.45	0.34
154	0.14	-0.29	-20.1	0.34	0.36
156	0.69	0.19	34.4	0.48	0.25
160	0.26	-0.11	40.7	0.35	0.37